Chemistry–A European Journal

Supporting Information

Shorter Alkyl Chains Enhance Molecular Diffusion and Electron Transfer Kinetics between Photosensitisers and Catalysts in CO_2-Reducing Photocatalytic Liposomes

David M. Klein, Santiago Rodríguez-Jiménez, Marlene E. Hoefnagel, Andrea Pannwitz, Amrutha Prabhakaran, Maxime A. Siegler, Tia E. Keyes, Erwin Reisner, Albert M. Brouwer, and Sylvestre Bonnet*

Table of contents

1. Methods

General methods. ^{1}H NMR and ^{13}C NMR spectra were recorded on a Bruker AV400 MHz spectrometer and ^{19}F NMR spectra on a Bruker AV500 MHz spectrometer. Chemical shift values (δ) are reported in ppm relative to the solvent. Electrospray ionisation mass spectrometry (ESI-MS) spectra were measured with a ThermoFischer Scientific MSQ Plus electrospray ionisation mass spectrometer with a 17 – 2000 *m/z* detection range and a resolution of approximately 0.5 *m/z*. High-resolution mass spectrometry (HRMS) was measured via direct injection on a Thermo Finnagan LTQ Orbitrap with electrospray ionisation. Elemental analysis was performed by Mikroanalytisches Laboratorium Kolbe in Oberhausen, Germany. UV-Vis absorption spectra were measured on a Varian Cary60 spectrophotometer equipped with a single cell Peltier temperature controller at 25 °C using either a 3 mL cuvette for standard solutions or a 0.6 mL cuvette for liposome solutions. Emission spectra were measured on a FLS900 spectrometer from Edinburgh Instruments Ltd. in a 3 mL cuvette at 22 °C using 380 nm as excitation source for the rhenium complexes and 450 nm as excitation source for the ruthenium complexes. Luminescence lifetimes were measured for rhenium complexes using the set-up for transient absorption spectroscopy described below, using an excitation wavelength of 380 nm. Instead of detecting the transmitted probe light, the spontaneous emission generated by the laser pulse was observed at different delay times determined by the electronically controlled detector gate (gate width = 5 ns), and the intensity versus time was modelled by a monoexponential decay using Glotaran.[1] Confocal microscopy images were taken on a Nikon Eclipse Ti microscope with 20x objective (0.75 NA, 1.00 WD) and confocal imaging with 488 nm laser and 640 – 680 nm detection wavelength. Images were processed with the Fiji version of ImageJ2.

Preparation of liposomes for immobilisation studies and photocatalysis. DMPC, DPPC, or DSPC lipids in chloroform, NaDSPE-PEG2K in chloroform, **RuC$_n$** in methanol, and/or **ReC$_n$** in chloroform were added in a pressure resistant tube. The organic solvents were evaporated under reduced pressure and the resulting lipid film was dried for at least 1 hour in *vacuo* to remove residual solvent. The film was then hydrated with NaH_2PO_4 buffer (4 mL, 0.1 M, pH = 7.7) with or without sodium ascorbate (0.1 M), followed by 10 freeze-thaw cycles in liquid N_2 and 50 °C water bath. Subsequently, the vesicles were extruded 11x with an Avanti Polar Lipids mini-extruder through a 0.2 µm polycarbonate membrane at 10 °C above the phase transition temperature of the lipid. Assuming no losses during preparation, the resulting liposomes consist of lipid:NaDSPE-PEG2K:**RuC$_n$**:**ReC$_n$** in the ratio 100:1.0:0.4:0.4 with expected bulk concentrations of 6.25 mM lipid, 0.625 mM NaDSPE-PEG2K, and 0.025 mM **RuC$_n$** and 0.025 mM **ReC$_n$**. Liposome samples were stored at RT and used within one week. For photocatalytic

CO_2 reduction experiments, the liposome solutions were diluted ten-fold with the same buffer as that used for liposome preparation. The size distribution of the hydrodynamic diameter (Z_{ave}) and the polydispersity index (PDI) were measured at 25 °C by dynamic light scattering with a Zetasizer Nano-S from Malvern operating at 632.8 nm with a scattering angle of 173°; at this wavelength neither **RuC_n** nor **ReC_n** absorb light significantly.

Photocatalysis measurements. Before photocatalysis, the liposome-containing solution obtained right after extrusion (0.3 mL) was diluted 10-fold using an aqueous solution containing 0.1 M phosphate buffer and 0.1 M sodium ascorbate. It was then purged in triplicates for 20 min with CO_2, or N_2 for control experiments, containing in both cases 2% methane as internal standard for gas chromatography. After purging, the vials were kept in a water bath at 25 °C and irradiated for 3 h using a Newport Oriel Xenon 150 W solar light simulator (100 mW cm^{-2}, AM1.5G containing infrared water and ultraviolet ($\lambda > 455$ or 400 nm) filters).

Product quantification. The amount of produced H_2 and CO was monitored by headspace gas analysis using a Shimadzu Tracera GC-2010 Plus with a barrier discharge ionisation detector. The GC-2010 Plus was equipped with a ShinCarbon micro-ST column (0.53 mm diameter) kept at 40 °C using helium carrier gas. Aliquots of 50 µL of the headspace gas were removed from the sealed photocatalytic vials using a gastight syringe (Hamilton) for gas chromatography analysis at hourly time intervals. Each different photocatalytic experiment was performed in triplicate, unless stated otherwise. Data are presented as mean ± standard error of the mean. The mean values and standard errors of the mean were calculated from the number of repeats of independent experiments.

Isotopic labelling experiment. Photocatalysis experiment with $^{13}CO_2$ as the headspace gas was performed. After three hours of simulated light irradiation, the vial headspace was transferred to an evacuated gas infrared cell (SpecAc, 10 cm path length, equipped with KBr windows) and a high-resolution transmission spectrum was collected on a Thermo Scientific Nicolet iS50 FT-IR spectrometer. To check whether formate had formed, an aliquot of the aqueous phase, together with a D_2O solution of trimethylsilylpropanoic acid as internal standard, was measured by ^1H NMR on a Bruker 400 MHz NMR spectrometer at room temperature.

Quantum yield measurements. One-millilitre solutions containing DPPC liposomes made of **ReC_9** and **RuC_9** (bulk concentration = 25 µM) were irradiated with monochromatic light (λ = 455 nm), using two different light intensities (I_1 = 10.5 mW cm^{-2}, and I_2 = 13.5 mW cm^{-2}), produced by a solar simulator (LOT LSN 254) equipped with a monochromator (LOT MSH 300). Duplicate experiments were

performed for each light intensity and the averaged values of the produced mol of CO were utilised to determine the Φ_{CO} using Equation S1:

$$\phi_{CO}\ (\%) = \frac{2\, n_{CO}\, N_A\, h\, c}{t_{irr}\, \lambda\, I\, A\, P} \cdot 100 \qquad \text{Equation S1}$$

where n_{CO} is the moles of photogenerated CO gas ($n_{CO,1}$ = 2.12 x 10^{-8} mol and $n_{CO,2}$ = 1.20 x 10^{-8} mol), N_A is the Avogadro constant in mol^{-1}, h is the Planck constant in J s, c the speed of light in m s^{-1}, t_{irr} is the irradiation time (3600 s), λ is the monochromatic light wavelength in m, I the light intensity in $J\ s^{-1}\ m^{-2}$, and A is the irradiation cross-section (1 x 10^{-4} m^2). P is the probability of absorbing a photon by the photosensitiser, i.e. $1 - 10^{-(Abs@454nm)}$, where due to the high scattering of the DPPC liposomes the absorbance used (0.252) was calculated employing the bulk concentration (25 µM), the extinction coefficient (1.32 x 10^4 M^{-1} cm^{-1}), and the immobilisation correction factor (η_{immob} = 0.764) of photosensitiser **RuC$_9$**.

Protocol for cyclic voltammetry (CV) and differential pulse voltammetry (DPV). CV and DPV were recorded with an Autolab Pgstat 10 potentiostat controlled by GPES4 software in a customised glass cell, equipped with a 1 mM solution of **RuC$_n$** or **ReC$_n$** and 0.1 M Bu_4NPF_6 in 6 mL dry acetonitrile or dichloromethane. The solution was stirred and degassed with argon for 15 minutes before each measurement. At the end of each measurement, 5 mg (0.03 mmol) ferrocene was added as an internal reference. A glassy carbon working electrode, a Ag/AgCl reference electrode, and a platinum counter electrode were employed to obtain spectra typically from -2.0 V to 1.6 V, with a scan rate of 100 mV/s (CV) or 50 mV/s (DPV).

Protocol for studying immobilisation efficiency of metal complexes on liposomes. For the immobilisation efficiency tests, liposome samples (0.6 mL) were loaded in specialised safe-lock Eppendorfs (Thermo Scientific X100 Tube PA Microtubes, 1.5 mL) and placed within adapters from Beranek Laborgeräte (catalogue number 11044). Subsequently, the liposomes were spinned down by ultracentrifugation on a Beckman Coulter Optima XE-90 Ultracentrifuge, using a Ti70 rotor at 36000 rpm (max. 100.4 kG) and 4 °C. Afterwards, the supernatant was separated from the pellet containing liposomes and immobilised metal complexes. Both the liposome stock sample before ultracentrifugation, as well as the supernatant were subsequently studied by UV-Vis spectroscopy and ICP-MS analysis.

Protocol for ICP-MS analysis. The supernatant samples for ICP-MS were prepared by digesting 100 µL supernatant sample in 100 µL nitric acid (65%) in a 10 mL plastic tube overnight. Then 9.8 mL MilliQ water was added. The solutions still containing liposomes were prepared by adding 100 µL liposome sample to 80 µL 37% HCl and 120 µL 65% HNO_3 in a glass tube with a glass marble on top and digesting for 48 hours at 90°C in the oven. After 48 hours the water had evaporated and 10 mL MilliQ water was added. The ruthenium and rhenium content of the samples were subsequently measured in triplicate using a NexION 2000 ICP mass spectrometer, a SC2 DX auto sampler, and Syngistix software from Perkin Elmer.

Nanosecond transient absorption spectroscopy. Nanosecond transient absorption was measured using an in-house assembled setup in which transient (ΔA) spectra were recorded as a function of delay time with respect to a laser pulse exciting the solution.[2] The excitation pulses at 450 nm (3.5 mJ/pulse; ca. 5 ns full width at half maximum) were generated using a tunable Nd:YAG-laser system (NT342B, Ekspla). The laser system was operated at a repetition rate of 5 Hz. The probe light, running at 10 Hz, was generated by a high-stability short arc xenon flash lamp (FX-1160, Excelitas Technologies) with a modified PS302 controller (EG&G). The probe light was split in a signal and a reference beam with a 50/50 beam splitter and focused on the entrance slit of a spectrograph (SpectraPro-150, Princeton Instruments). The probe beam (A = 1 mm^2) was passed through the sample cell and orthogonally overlapped with the excitation beam on a 1 mm × 1 cm area. The excitation power was recorded by measuring the excitation power at the back of an empty sample holder. The reference beam was used to normalise the signal for fluctuations in the flash lamp spectral intensity. Both beams were recorded simultaneously using a gated intensified CCD camera (PI-MAX3, Princeton Instruments) with an adjustable gate (gate width = 20 ns). The timing of the excitation pulse, the flash lamp, and the gate of the camera was achieved with a delay generator (DG645, Stanford Research Systems, Inc.). The setup was controlled by an in-house written program (LabView). Spectra were averaged from 490 to 540 nm (**RuC$_n^-$** absorption) and the ΔA_{av} values as a function of time were fitted with Equation 5 using Igor Pro version 8 (Wavemetrics).

Microcavity Support. The micropore array substrates for fluorescence correlation spectroscopy were prepared in polydimethylsiloxane (PDMS) as described previously.[3] First, mica sheets were cut in to 1 cm^2 area and glued to a cover glass slide. ~20 µL of ethanolic solution of 0.1% of 4.61 µm polystyrene spheres was drop cast onto the flat mica sheet and after evaporation, PDMS was poured over the array of spheres, and cured at 90 °C for 1 h. On cooling, the PDMS was gently peeled off to create a thin chamber of identical dimensions of mica sheet thickness. The pores were generated by dissolving PS sphere from the PDMS substrate by immersion and sonication in tetrahydrofuran for 15 min. The

substrates were then left to dry overnight. The PDMS substrates were then plasma cleaned using oxygen plasma for 5 min to make the surface hydrophilic and the microcavities were buffer filled by sonication and stored inside buffer prior to applying the bilayer.

Preparation of microcavity supported lipid bilayers. The lipid bilayers were prepared on the PDMS substrate containing 2 µm sized cavities through Langmuir-Blodgett technique followed by vesicle fusion methods.[3] The proximal lipid monolayer was transferred by Langmuir-Blodgett technique (KSV Nema) in the air-water interface. The lipid solution was left to evaporate for about 10 min at the sub-phase surface (MilliQ water, pH 7.4) and the lipid monolayer was transferred at a surface pressure of 40 mN/m. The liposomes were prepared by mixing DPPC:NaDSPE-PEG2K:**RuC$_n$** in the ratio $100:1:4\cdot10^{-4}$ and then it was dried under nitrogen flow. It was kept under vacuum for 60 minutes and hydrated using phosphate buffer saline (pH 7.7) followed by vortex agitation. These vesicles were extruded with 0.2 µm polycarbonate membrane at 10 °C above the phase transition temperature of the lipid. These vesicles were injected to the microfluidic chamber of lipid monolayer. It was allowed to fuse for 90 min and the residual liposomes were removed by phosphate buffer saline wash.

Fluorescence lifetime correlation spectroscopy (FLCS). The diffusion coefficient of **RuC$_n$**-labelled supported lipid bilayers were obtained using FLCS, accomplished on a MicroTime 200 system (Picoquant GmBH, Berlin, Germany) consisting of an inverted Olympus X1-71 microscope with an Olympus UPlanSApo 60x/1.2 water immersion objective, a time correlated single photon counting (TCSPC) unit, and a dual single photo avalanche diode (SPAD). The **RuC$_n$** probes were excited with a 532 nm laser PicoTA from Toptica (Picoquant) with a pulse repetition rate of 20 MHz. 532 nm was selected as the excitation wavelength as it gave superior S/N ratio in the time trace due to reflectance from the substrate at 440 nm. The excitation light was directed onto the sample through the objective lens by a 440/532rpc dichroic mirror. The emitted fluorescence was also collected through the same objective and filtered by the dichroic mirror and by a 580 nm interference filter. A 50 µm pinhole was used in order to confine the detection volume in the axial direction onto the SPAD. The autocorrelation functions (ACFs) were fitted using Equation S2:

$$G(\tau) = \left[\frac{1}{N}\right]\left[\frac{1}{1+\left(\frac{\tau}{\tau_{D1}}\right)^{\alpha_1}}\right] + \left[\frac{(1-c)}{\left(1+\frac{\tau}{\tau_{D2}}\right)^{\alpha_2}}\right] \qquad \text{Equation S2}$$

where G(τ) is the autocorrelation function of fluorescence fluctuations, N is the average number of diffusing fluorophores in the effective volume, τ is the delay time, τ_{D1} and τ_{D2} are the diffusion time of

the molecules across the confocal volume of the 1st component and 2nd component respectively, α_1 and α_2 are the anomalous parameters of the 1st and 2nd components, respectively, and c is the contribution of the diffusing species. ACFs were fitted using the two-dimensional model of diffusion to determine the diffusion time and the diffusion coefficient was calculated using Equation S3:

$$D = \frac{\omega^2}{4\tau_D} \qquad \text{Equation S3}$$

where D is the diffusion coefficient and ω is the $1/e^2$ radius of the confocal volume. ω was measured using ATTO-532 (Atto TEC, GmbH) dye solution of known diffusion coefficient at 20 °C in water. All measurements were performed with a dye concentration of 10 nM. Three-dimensional diffusion of 10 nM **RuC_{19}** was recorded in acetonitrile and the ACF was fitted using the three-dimensional diffusion model:

$$G(\tau) = \left[\frac{1}{N}\right]\left[\frac{1}{1+\left(\frac{\tau}{\tau_D}\right)^{\alpha}}\right]\left[\frac{1}{\sqrt{1+\left(\frac{\tau}{\tau_D}\right)^{\alpha} K^2}}\right] \qquad \text{Equation S4}$$

where K is the length to diameter ratio of the confocal volume. The fluorescence lifetime image was also taken in the same MicroTime 200 system. Each sample was acquired for 360 s with a 512 x 512 resolution. Data was analysed using PicoQuant Symphotime software.

2. Synthesis

Materials and reagents. Chemical reagents and solvents were purchased from commercial suppliers and were used without further purification. Sodium ascorbate (≥ 99%) and $NaH_2PO_4 \cdot 2H_2O$ were purchased from Merck. 2,2'-bipyridine (bpy), 4,4'-dionyl-bpy, $[Re(CO)_5Cl]$, and bpy-$(C_9)_2$ were purchased from Sigma Aldrich. The lipids (dry powder) 1,2-dimyristoyl-*sn*-glycero-3-phosphocholine (DMPC), 1,2-dipalmitoyl-*sn*-glycero-3-phosphocholine (DPPC), 1,2-distearoyl-*sn*-glycero-3-phosphocholine (DSPC) were purchased from Avanti Polar Lipids and stored at −20 °C. Sodium 1,2-distearoyl-*sn*-glycero-3-phosphoethanolamine N-(carbonyl-methoxypolyethylene glycol-2000) (NaDSPE-PEG2K) was purchased from Lipoid and stored at −20 °C. *cis*-$[Ru(bpy)_2Cl_2]$ was synthesised according to literature, while isolating $[Ru(bpy)_3](PF_6)_2$ as a side product after anion exchange with potassium hexafluorophosphate.[4] Phosphate buffer (1 L, 0.1 M, pH = 7.7) was prepared by dissolving $NaH_2PO_4 \cdot 2H_2O$ (12 g) in Milli-Q water (500 mL), adjusting the pH with NaOH (≈ 90 mL, 1 M), and diluting further with Milli-Q water up to 1 L. The Avanti Mini-Extruder including polycarbonate extrusion filter (pore size = 0.2 µm, diameter = 19 mm) and filter supports (10 mm) was purchased from Avanti Polar Lipids.

General procedure for the synthesis of 4,4'-$(C_nH_{2n+1})_2$-bpy. 4,4'-$(C_nH_{2n+1})_2$-bpy (n = 12, 15, 17, and 19) were synthesised according to a known procedure for **4,4'-$(C_9H_{19})_2$-bpy**.[5] Tetrahydrofuran was dried over 3 Å molecular sieves overnight and was deoxygenated under N_2 prior to use. To a solution of diisopropylamine (2.4 mM in tetrahydrofuran, 2.7 equiv.) was added a solution of *n*-butyllithium (1.6 M or 2.5 M in hexane, 2.7 equiv.) under N_2 atmosphere. After 1 h at 0 °C, 4,4'-dimethyl-2,2'-bipyridine (0.14 mM in tetrahydrofuran, 1.0 equiv.) was added dropwise to the yellow solution. After another 3 h at 0 °C, 1-bromoundecane (1.4 mM in tetrahydrofuran, 2.7 equiv.) was added dropwise to the red solution and the solution was allowed to warm to room temperature. After 1 day, the reaction mixture was quenched with water. The aqueous phase was extracted with diethyl ether (3 x). The combined organic phases were dried over $MgSO_4$, the dried solution was filtered, and the filtrate was concentrated under reduced pressure. The crude product **4,4'-$(C_nH_{2n+1})_2$-bpy** was either recrystallised from pentane (n = 12, 15, and 17) or it was collected by filtration after it precipitated during extraction (n = 19).

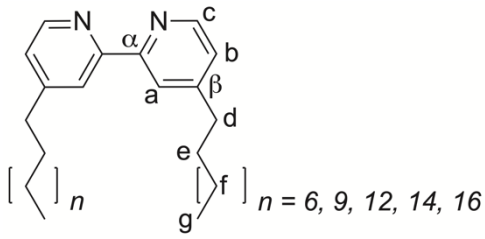

4,4'-didodecyl-2,2'-bipyridine (4,4'-($C_{12}H_{25}$)$_2$-bpy): method above, from 4,4'-dimethyl-2,2'-bipyridine (2.0 g, 10.9 mmol); white solid (yield: 3.2 g, 6.5 mmol, 60%). R_f = 0.7 (SiO_2, DCM/MeOH 9:1). ^{1}H NMR (400 MHz, $CDCl_3$): δ = 8.58 (d, *J* = 5.0 Hz, 2H, *c*), 8.26 (s, 2H, *a*), 7.16 (dd, *J* = 5.0, 1.5 Hz, 2H, *b*), 2.71 (t, *J* = 7.6 Hz, 4H, *d*), 1.71 (p, *J* = 7.6 Hz, 4H, *e*), 1.27 (m, 36H, *f*), 0.90 (t, *J* = 6.7 Hz, 6H, *g*). ^{13}C NMR (100 MHz, $CDCl_3$): δ = 156.09 (C_q, *α*), 153.20 (C_q, *β*), 149.00 (CH, *c*), 124.08 (CH, *b*), 121.51 (CH, *a*), 35.69 (CH_2, *d*), {32.05, 30.60, 29.79 – 29.45, 22.82 (CH_2, *e+f*)}, 14.25 (CH_3, *g*). HRMS (ESI) *m/z* found (calcd): 493.45146 (493.45163, [*M*+H]$^+$). Elemental analysis calcd (%) for $C_{34}H_{56}N_2 \cdot H_2O$: C 79.94, H 11.44, N 5.48; found: C 80.47, H 11.37, N 5.31.

4,4'-dipentadecyl-2,2'-bipyridine (4,4'-($C_{15}H_{31}$)$_2$-bpy): method above, from 4,4'-dimethyl-2,2'-bipyridine (1.0 g, 5.4 mmol); white solid (yield: 1.2 g, 2.0 mmol, 37%). ^{1}H NMR (400 MHz, $CDCl_3$): δ = 8.56 (d, *J* = 5.0 Hz, 2H, *c*), 8.26 (s, 2H, *a*), 7.15 (dd, *J* = 5.0, 1.5 Hz, 2H, *b*), 2.69 (t, *J* = 7.8 Hz, 4H, *d*), 1.69 (p, *J* = 7.8 Hz, 4H, *e*), 1.25 (m, 48H, *f*), 0.87 (t, *J* = 6.8 Hz, 6H, *g*). ^{13}C NMR (100 MHz, $CDCl_3$): δ = 155.77 (C_q, *α*), 153.51 (C_q, *β*), 148.85 (CH, *c*), 124.19 (CH, *b*), 121.69 (CH, *a*), 35.72 (CH_2, *d*), {32.07, 30.59, 29.85-29.45, 22.84 (CH_2, *e+f*)}, 14.27 (CH_3, *g*). HRMS (ESI) *m/z* found (calcd): 577.54527 (577.54553, [*M*+H]$^+$). Elemental analysis calcd (%) for $C_{40}H_{68}N_2$: C 83.27, H 11.88, N 4.86; found: C 83.23, H 11.94, N 4.82.

4,4'-diheptadecyl-2,2'-bipyridine (4,4'-($C_{17}H_{35}$)$_2$-bpy): method above, from 4,4'-dimethyl-2,2'-bipyridine (2.0 g, 10.9 mmol); white solid (yield: 2.2 g, 3.5 mmol, 32%). ^{1}H NMR (400 MHz, $CDCl_3$): δ = 8.55 (d, *J* = 5.3 Hz, 2H, *c*), 8.23 (d, *J* = 1.5 Hz, 2H, *a*), 7.13 (dd, *J* = 5.3, 1.5 Hz, 2H, *b*), 2.68 (t, *J* = 6.8 Hz, 4H, *d*), 1.68 (p, *J* = 6.5 Hz, 4H, *e*), 1.25 (m, 56H, *f*), 0.87 (t, *J* = 6.7 Hz, 6H, *g*). ^{13}C NMR (100 MHz, $CDCl_3$): δ = 156.23 (C_q, *α*), 153.14 (C_q, *β*), 149.07 (CH, *c*), 124.07 (CH, *b*), 121.49 (CH, *a*), 35.70 (CH_2, *d*), {32.07, 30.62, 29.84, 29.82, 29.80, 29.78, 29.68, 29.58, 29.51, 29.48, 22.84 (CH_2, *e+f*)}, 14.27 (CH_3, *g*). MS (ESI) *m/z* found (calcd): 633.6 (633.6, [*M*+H]$^+$). Elemental analysis calcd (%) for $C_{44}H_{76}N_2$: C 83.47, H 12.10, N 4.42; found: C 83.43, H 12.07, N 4.39. Colourless single crystals of **4,4'-($C_{17}H_{35}$)$_2$-bpy** were obtained by evaporation of the solvent $CDCl_3$ at room temperature. The structure and refinement data are shown in the section on single crystal X-ray crystallography.

4,4'-dinonadecyl-2,2'-bipyridine (4,4'-($C_{19}H_{39}$)$_2$-bpy): method above, from 4,4'-dimethyl-2,2'-bipyridine (2.0 g, 10.9 mmol); white solid (yield: 3.5 g, 5.0 mmol, 46%). R_f = 0.4 (SiO_2, pentane/EtOAc

10:1). ^{1}H NMR (400 MHz, $CDCl_3$): δ = 8.56 (d, *J* = 5.0 Hz, 2H, *c*), 8.24 (s, 2H, *a*), 7.14 (dd, *J* = 5.0, 1.7 Hz, 2H, *b*), 2.69 (t, *J* = 7.6 Hz, 4H, *d*), 1.68 (p, *J* = 7.6 Hz, 4H, *e*), 1.25 (m, 64H, *f*), 0.86 (t, *J* = 6.8 Hz, 6H, *g*). ^{13}C NMR (100 MHz, $CDCl_3$): δ = 156.02 (C_q, *α*), 153.31 (C_q, *β*), 148.98 (CH, *c*), 124.12 (CH, *b*), 121.57 (CH, *a*), 35.71 (CH_2, *d*), {32.07, 30.61, 29.86-29.46, 22.84 (CH_2, *e+f*)}, 14.27 (CH_3, *g*). HRMS (ESI) *m/z* found (calcd): 689.66953 (689.67073, $[M+H]^+$). Elemental analysis calcd (%) for $C_{48}H_{84}N_2 \cdot 0.5\ H_2O$: C 82.57, H 12.27, N 4.01; found: C 82.60, H 12.12, N 3.99.

General procedure for the synthesis of [Re(4,4'-(C_nH_{2n+1})$_2$-bpy)(CO)$_3$Cl] (ReC$_n$): The compounds were synthesised according to known procedures.[6,7] To a solution of $[Re(CO)_5Cl]$ (typically 0.028 mM in dry toluene, 1.0 equiv. or 1.5 equiv., respectively, in case of **ReC$_{19}$**) was added **4,4'-(C_nH_{2n+1})$_2$-bpy** (1.0 equiv.) under inert atmosphere and the yellow mixture was heated to reflux. After 3 – 48 h, the orange solution was concentrated under reduced pressure. The residue was redissolved in a minimum amount of diethyl ether and the solution was carefully concentrated until the desired product started to precipitate, which was collected by vacuum filtration. Due to the alkyl chain length, different procedures were followed from this point. For **ReC$_9$** and **ReC$_{12}$**, concentration of the filtrate resulted in additional solids, which were reprecipitated by dissolving in acetone and evaporation under reduced pressure. For **ReC$_{15}$** and **ReC$_{17}$**, the precipitate was washed with 3 x 20 mL acetone and vacuum dried. For **ReC$_{19}$**, the precipitate was washed with 3 x 20 mL Et_2O and vacuum dried.

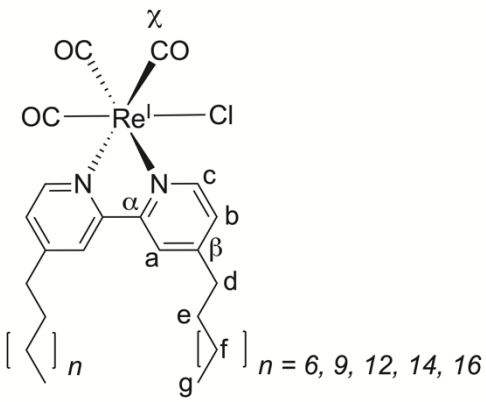

[Re(bpy)(CO)$_3$Cl] (ReC$_0$): from $[Re(CO)_5Cl]$ (81 mg, 0.22 mmol) and bpy (35 mg, 0.22 mmol); yellow solid (yield: 86 mg, 0.19 mmol, 83%). Elemental analysis calcd (%) for $C_{13}H_8N_2O_3ReCl$: C 33.81, H 1.75, N 6.07; found: C 33.67, H 1.74, N 5.99.

[Re(4,4'-(C_9H_{19})$_2$-bpy)(CO)$_3$Cl] (ReC$_9$): from $[Re(CO)_5Cl]$ (100 mg, 0.28 mmol) and **4,4'-(C_9H_{19})$_2$-bpy** (113 mg, 0.28 mmol); yellow solid **ReC$_9$** (yield: 195 mg, 0.27 mmol, 99%). ^{1}H NMR (400 MHz, $CDCl_3$): δ = 8.88 (d, *J* = 5.7 Hz, 2H, *c*), 7.95 (s, 2H, *a*), 7.32 (dd, *J* = 5.7, 1.6 Hz, 2H, *b*), 2.78 (t, *J* = 7.7 Hz, 4H, *d*), 1.70 (p, *J* = 7.7 Hz, 4H, *e*), 1.28 (m, 24H, *f*), 0.88 (t, *J* = 6.7 Hz, 6H, *g*). ^{13}C NMR (100 MHz, $CDCl_3$): δ = 197.44 (CO), 190.05 (CO), 156.00 (C_q, *α*), 155.63 (C_q, *β*), 152.77 (CH, *c*), 127.23 (CH, *b*), 123.13 (CH, *a*), 35.84 (CH_2,

d), {31.95, 30.33, 29.55, 29.48, 29.38, 22.77 (CH_2, *e+f*)}, 14.23 (CH_3, *g*). UV-Vis ($CHCl_3$): λ_{max} (ε): 382 nm (3.86×10^3 $mol^{-1}dm^3cm^{-1}$). Phosphorescence ($CHCl_3$): λ_{ex} = 380 nm, λ_{em} = 582 nm, τ = 76 ns. HRMS (ESI) *m/z* found (calcd): 679.28924 (679.29039, [*M*-Cl]$^+$), 720.31590 (720.31699, [*M*-Cl+CH_3CN]$^+$), 732.29069 (732.29350, [*M*+NH_4]$^+$), 737.24709 (737.24824, [*M*+Na]$^+$). Elemental analysis calcd (%) for $C_{31}H_{44}N_2O_3ReCl$: C 52.12, H 6.21, N 3.92; found: C 52.10, H 6.22, N 3.94.

[Re(4,4'-($C_{12}H_{25}$)$_2$-bpy)(CO)$_3$Cl] (ReC_{12}): from $[Re(CO)_5Cl]$ (100 mg, 0.28 mmol) and **4,4'-($C_{12}H_{25}$)$_2$-bpy** (136 mg, 0.28 mmol); yellow solid **ReC_{12}** (yield: 146 mg, 0.18 mmol, 67%). ^{1}H NMR (400 MHz, $CDCl_3$): δ = 8.88 (d, *J* = 5.7 Hz, 2H, *c*), 7.96 (s, 2H, *a*), 7.32 (dd, *J* = 5.7, 1.7 Hz, 2H, *b*), 2.78 (t, *J* = 7.6 Hz, 4H, *d*), 1.70 (p, *J* = 7.6 Hz, 4H, *e*), 1.27 (m, 36H, *f*), 0.87 (t, *J* = 6.7 Hz, 6H, *g*). ^{13}C NMR (100 MHz, $CDCl_3$): δ = 197.45 (CO), 190.02 (CO), 156.01 (C_q, α), 155.61 (C_q, β), 152.74 (CH, *c*), 127.22 (CH, *b*), 123.14 (CH, *a*), 35.83 (CH_2, *d*), {32.02, 30.32, 29.75, 29.73, 29.60, 29.48, 29.46, 29.39, 22.80 (CH_2, *e+f*)}, 14.24 (CH_3, *g*). UV-Vis ($CHCl_3$): λ_{max} (ε): 383 nm (3.98×10^3 $mol^{-1}dm^3cm^{-1}$). Phosphorescence ($CHCl_3$): λ_{ex} = 380 nm, λ_{em} = 588 nm, τ = 74 ns. HRMS (ESI) *m/z* found (calcd): 763.38378 (763.38434, [*M*-Cl]$^+$), 804.41072 (804.41088, [*M*-Cl+CH_3CN]$^+$), 816.38649 (816.38752, [*M*+NH_4]$^+$), 821.34191 (821.34219, [*M*+Na]$^+$). Elemental analysis calcd (%) for $C_{37}H_{56}N_2O_3ReCl \cdot 2\ C_3H_6O$: C 56.47, H 7.49, N 3.06; found: C 56.19, H 7.37, N 3.08.

[Re(4,4'-($C_{15}H_{31}$)$_2$-bpy)(CO)$_3$Cl] (ReC_{15}): from $[Re(CO)_5Cl]$ (107 mg, 0.30 mmol) and **4,4'-($C_{15}H_{31}$)$_2$-bpy** (170 mg, 0.30 mmol); yellow solid **ReC_{15}** (yield: 92 mg, 0.10 mmol, 35%). ^{1}H NMR (400 MHz, $CDCl_3$): δ = 8.89 (d, *J* = 5.7 Hz, 2H, *c*), 7.95 (s, 2H, *a*), 7.32 (dd, *J* = 5.7, 1.6 Hz, 2H, *b*), 2.78 (t, *J* = 7.7 Hz, 4H, *d*), 1.70 (p, *J* = 7.6 Hz, 4H, *e*), 1.26 (m, *J* = 6.6 Hz, 48H, *f*), 0.87 (t, *J* = 6.7 Hz, 6H, *g*). ^{13}C NMR (100 MHz, $CDCl_3$): δ = 197.44 (CO), 190.05 (CO), 155.99 (C_q, α), 155.63 (C_q, β), 152.79 (CH, *c*), 127.23 (CH, *b*), 123.13 (CH, *a*), 35.86 (CH_2, *d*), {32.05, 30.34, 29.82, 29.80, 29.79, 29.77, 29.75, 29.62, 29.49, 29.41, 22.82 (CH_2, *e+f*)}, 14.10 (CH_3, *g*). UV-Vis ($CHCl_3$): λ_{max} (ε): 382 nm (3.80×10^3 $mol^{-1}dm^3cm^{-1}$). Phosphorescence ($CHCl_3$): λ_{ex} = 380 nm, λ_{em} = 585 nm, τ = 74 ns. HRMS (ESI) *m/z* found (calcd): 847.47678 (847.47820, [*M*-Cl]$^+$), 888.50452 (888.50475, [*M*-Cl+CH_3CN]$^+$), 900.48034 (900.48142, [*M*+NH_4]$^+$), 905.43608 (905.43682, [*M*+Na]$^+$). Elemental analysis calcd (%) for $C_{43}H_{68}N_2O_3ReCl$: C 58.51, H 7.76, N 3.17; found: C 58.47, H 7.82, N 3.14.

[Re(4,4'-($C_{17}H_{35}$)$_2$-bpy)(CO)$_3$Cl] (ReC_{17}): from $[Re(CO)_5Cl]$ (88 mg, 0.24 mmol) and **4,4'-($C_{17}H_{35}$)$_2$-bpy** (153 mg, 0.24 mmol); yellow solid **ReC_{17}** (yield: 194 mg, 0.21 mmol, 85%). ^{1}H NMR (400 MHz, $CDCl_3$): δ = 8.89 (d, *J* = 5.8 Hz, 2H, *c*), 7.95 (s, 2H, *a*), 7.32 (dd, *J* = 5.7, 1.1 Hz, 2H, *b*), 2.78 (t, *J* = 7.8 Hz, 4H, *d*), 1.71 (p, *J* = 7.8 Hz, 4H, *e*), 1.26 (m, 56H, *f*), 0.88 (t, *J* = 6.9 Hz, 6H, *g*). ^{13}C NMR (100 MHz, $CDCl_3$) δ = 197.43

(CO), 190.06 (CO), 155.98 (C_q, *α*), 155.63 (C_q, *β*), 152.79 (CH, *c*), 127.23 (CH, *b*), 123.12 (CH, *a*), 35.86 (CH_2, *d*), {32.06, 30.19, 29.83, 29.81, 29.79, 29.76, 29.63, 29.50, 29.41, 22.82 (CH_2, *e+f*)}, 14.10 (CH_3, *g*). UV-Vis ($CHCl_3$): λ_{max} (ε): 383 nm (3.83×10^3 $mol^{-1}dm^3cm^{-1}$). Phosphorescence ($CHCl_3$): λ_{ex} = 380 nm, λ_{em} = 581 nm, τ = 74 ns. HRMS (ESI) *m/z* found (calcd): 903.53904 (903.54109, $[M\text{-Cl}]^+$), 944.56588 (944.56766, $[M\text{-Cl+CH}_3\text{CN}]^+$), 956.54294 (956.54341, $[M\text{+NH}_4]^+$), 961.49829 (961.49881, $[M\text{+Na}]^+$). Elemental analysis calcd (%) for $C_{47}H_{76}N_2O_3ReCl$: C 60.13, H 8.16, N 2.98; found: C 60.15, H 8.22, N 2.95.

[Re(4,4'-($C_{19}H_{39}$)$_2$-bpy)(CO)$_3$Cl] (ReC_{19}): from $[Re(CO)_5Cl]$ (157 mg, 0.44 mmol) and **4,4'-($C_{19}H_{39}$)$_2$-bpy** (200 mg, 0.29 mmol); yellow solid **ReC_{19}** (yield: 161 mg, 0.16 mmol, 56%). ^{1}H NMR (400 MHz, $CDCl_3$): δ = 8.87 (d, *J* = 5.7 Hz, 2H, *c*), 7.96 (s, 2H, *a*), 7.31 (dd, *J* = 5.7, 1.4 Hz, 2H, *b*), 2.77 (t, *J* = 7.6 Hz, 4H, *d*), 1.70 (p, *J* = 7.6 Hz, 4H, *e*), 1.25 (m, 64H, *f*), 0.87 (t, *J* = 6.7 Hz, 6H, *g*). ^{13}C NMR (100 MHz, $CDCl_3$): δ = 197.45 (CO), 189.99 (CO), 156.01 (C_q, *α*), 155.59 (C_q, *β*), 152.69 (CH, *c*), 127.19 (CH, *b*), 123.16 (CH, *a*), 35.80 (CH_2, *d*), {32.02, 30.30, 29.80, 29.76, 29.73, 29.60, 29.47, 29.37, 22.79 (CH_2, *e+f*)}, 14.23 (CH_3, *g*). UV-Vis ($CHCl_3$): λ_{max} (ε): 381 nm (3.80×10^3 $mol^{-1}dm^3cm^{-1}$). HRMS (ESI) *m/z* found (calcd): 1007.56265 (1007.56146, $[M\text{+Na}]^+$), 1002.60725 (1002.60606, $[M\text{+NH}_4]^+$). Elemental analysis calcd (%) for $C_{51}H_{84}ClN_2O_3Re$: C 61.57, H 8.51, N 2.82; found: C 60.93, H 8.38, N 2.76.

General procedure for [Ru(4,4'-(C_nH_{2n+1})$_2$-bpy)(bpy)$_2$](PF_6)$_2$ (RuC_n): The synthesis for **RuC_n** was followed as reported in literature for a similar compound with some modifications.[5] To a solution of *cis*-$[Ru(bpy)_2Cl_2]$ (typically 0.014 mM in deoxygenated water/ethanol = 1:1 for **RuC_9** and **RuC_{12}** or water/ethanol/chloroform = 1:1:1 for **RuC_{15}**, **RuC_{17}**, and **RuC_{19}**, 1.0 equiv.) was added the respective **4,4'-(C_nH_{2n+1})$_2$-bpy** (1.0 equiv.) and the reaction mixture was heated to reflux at 110 °C under inert atmosphere. After 1 – 4 days, the reaction mixture was concentrated under reduced pressure. The crude product was purified as described in the following protocols.

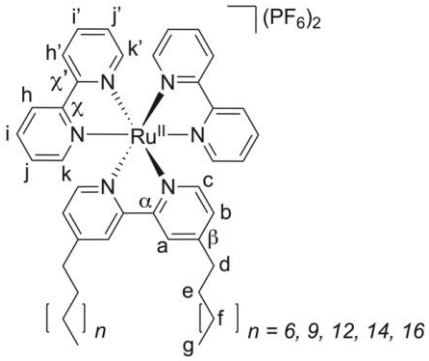

[Ru(bpy)$_3$](PF_6)$_2$ (RuC_0): Elemental analysis calcd (%) for $C_{30}H_{24}F_{12}N_6P_2Ru$: C 41.92, H 2.81, N 9.78; found: C 41.56, H 2.84, N 9.72.

[Ru(4,4'-(C_9H_{19})$_2$-bpy)(bpy)$_2$](PF_6)$_2$ (RuC_9): from *cis*-[Ru(bpy)$_2$Cl$_2$] (0.22 g, 0.44 mmol) and **4,4'-(C_9H_{19})$_2$-bpy** (0.18 g, 0.44 mmol). For purification, the crude product was dissolved in a minimum amount of water. Saturated aqueous potassium hexafluorophosphate was added and the resulting orange precipitate was collected by vacuum filtration. The precipitate was dried by co-evaporation with toluene and *in vacuo*. **RuC_9** was obtained as a red solid (yield: 450 mg, 0.40 mmol, 91%). R_f = 0.6 (SiO_2, acetone/water/saturated KNO_3 100:10:1). ^{1}H NMR (400 MHz, CD_3CN): δ = 8.49 (d, *J* = 8.2 Hz, 4H, *h+h'*), 8.37 (s, 2H, *a*), 8.04 (t, *J* = 8.0, 2.9 Hz, 4H, *i+i'*), 7.72 (d, *J* = 5.2 Hz, 4H, *k+k'*), 7.54 (d, *J* = 5.5 Hz, 2H, *c*), 7.39 (q, *J* = 6.7 Hz, 4H, *j+j'*), 7.22 (d, *J* = 5.5 Hz, 2H, *b*), 2.79 (t, *J* = 7.8 Hz, 4H, *d*), 1.68 (p, *J* = 7.0 Hz, 4H, *e*), 1.27 (m, 24H, *f*), 0.87 (t, *J* = 6.4 Hz, 6H, *g*). ^{13}C NMR (100 MHz, CD_3CN): δ = 157.97 (C_q), 157.55 (C_q), 155.76 (C_q), 152.59 (CH, *k or k'*), 152.41 (CH, *k or k'*), 151.78 (CH, *c*), 138.51 (CH, *i+i'*), 128.46 (CH, *b, j or j'*), 128.42 (CH, *b, j or j'*), 128.40 (CH, *b, j or j'*), 125.15 (CH, *a*), 125.10 (CH, *h or h'*), 35.64 (CH_2, *d*), {32.51, 30.81, 30.08, 29.93, 29.90, 29.74, 23.30 (CH_2, *e+f*)}, 14.32 (CH_3, *g*). ^{19}F NMR (471 MHz, CD_3CN): δ = -72.77 (d, *J* = 706.7 Hz). UV-Vis (CH_3CN): λ_{max} (ε): 453 nm (1.32×10^4 $mol^{-1}dm^3cm^{-1}$). Phosphorescence (CH_3CN): λ_{ex} = 450 nm, λ_{em} = 617 nm. HRMS (ESI) *m/z* found (calcd): 411.19560 (411.19585, [*M*-2(PF_6)]$^{2+}$). Elemental analysis calcd (%) for $C_{48}H_{60}F_{12}N_6P_2Ru \cdot 3\ H_2O$: C 49.44, H 5.70, N 7.21; found: C 49.67, H 5.40, N 7.23.

[Ru(4,4'-($C_{12}H_{25}$)$_2$-bpy)(bpy)$_2$](PF_6)$_2$ (RuC_{12}): from *cis*-[Ru(bpy)$_2$Cl$_2$] (0.20 g, 0.41 mmol) and **4,4'-($C_{12}H_{25}$)$_2$-bpy** (0.20 g, 0.41 mmol. For purification, the procedure for **RuC_9** was followed. The orange precipitate was further purified by column chromatography on silica gel (dichloromethane/methanol = 99:1 to 90:10). The solvents were removed under reduced pressure and the remaining solids were dried *in vacuo*. **RuC_{12}** was obtained as a red solid (yield: 176 mg, 0.15 mmol, 36%). R_f = 0.6 (SiO_2, acetone/water/saturated KNO_3 100:10:1). ^{1}H NMR (400 MHz, CD_3CN): δ = 8.48 (dd, *J* = 8.2, 1.9 Hz, 4H, *h+h'*), 8.37 (d, *J* = 1.8 Hz, 2H, *a*), 8.04 (tq, *J* = 8.0, 2.8, 1.5 Hz, 4H, *i+i'*), 7.71 (dd, *J* = 5.2, 1.2 Hz, 4H, *k+k'*), 7.53 (d, *J* = 5.8 Hz, 2H, *c*), 7.38 (dq, *J* = 7.2, 5.6, 1.3 Hz, 4H, *j+j'*), 7.22 (dd, *J* = 5.8, 1.8 Hz, 2H, *b*), 2.78 (t, *J* = 7.6 Hz, 4H, *d*), 1.68 (p, *J* = 7.4 Hz, 4H, *e*), 1.25 (m, 36H, *f*), 0.87 (t, *J* = 6.9 Hz, 6H, *g*). ^{13}C NMR (100 MHz, CD_3CN): δ = 158.00 (C_q), 157.98 (C_q), 157.56 (C_q), 155.78 (C_q), 152.61 (CH, *k or k'*), 152.42 (CH, *k or k'*), 151.80 (CH, *c*), 138.53 (CH, *i+i'*), 128.50 (CH, *b, j or j'*) 128.44 (CH, *b, j or j'*), 125.15 (CH, *a*), 125.11 (CH, *h+h'*), 35.65 (CH_2, *d*), {32.58, 30.81, 30.32, 30.30, 30.24, 30.12, 30.02, 29.93, 29.74, 23.33 (CH_2, *e+f*)}, 14.35 (CH_3, *g*). ^{19}F NMR (471 MHz, CD_3CN): δ = -72.33 (d, *J* = 706.2 Hz). UV-Vis (CH_3CN): λ_{max} (ε): 453 nm (1.35×10^4 $mol^{-1}dm^3cm^{-1}$). Phosphorescence (CH_3CN): λ_{ex} = 450 nm, λ_{em} = 616 nm. HRMS (ESI) *m/z* found (calcd): 453.24253 (453.24289, [*M*-2(PF_6)]$^{2+}$). Elemental analysis calcd (%) for $C_{54}H_{72}F_{12}N_6P_2Ru$: C 54.22, H 6.07, N 7.03; found: C 53.67, H 6.04, N 6.82.

[Ru(4,4'-($C_{15}H_{31}$)$_2$-bpy)(bpy)$_2$](PF_6)$_2$ (RuC_{15}): from *cis*-[Ru(bpy)$_2$Cl$_2$] (0.21 g, 0.43 mmol) and **4,4'-($C_{15}H_{31}$)$_2$-bpy** (0.25 g, 0.43 mmol). For purification, the crude product was purified via chromatography on silica gel (acetone/water/brine = 8:4:1). The solvents were removed under reduced pressure and the red solid was extracted with chloroform (3 x). The combined organic layers were dried over $MgSO_4$ and the solvents were evaporated under reduced pressure. Methanol was added and the white precipitate was filtered off. Henceforth, the procedure for **RuC_9** was followed. The orange precipitate was collected by dissolving in acetone and dried by evaporation under reduced pressure and *in vacuo*. The yield in crude product before addition of hexafluorophosphate was 56% (258 mg, 0.24 mmol). From 105 mg of such crude product, KPF_6 reprecipitation afforded **RuC_{15}** as a red solid in 36% overall yield (82 mg, 0.064 mmol). ^{1}H NMR (400 MHz, CD_3CN): δ = 8.49 (d, *J* = 8.3 Hz, 4H, *h+h'*), 8.36 (d, *J* = 1.8 Hz, 2H, *a*), 8.04 (tt, *J* = 8.0, 1.8 Hz, 4H, *i+i'*), 7.71 (dd, *J* = 5.7, 1.4 Hz, 4H, *k+k'*), 7.53 (d, *J* = 5.8 Hz, 2H, *c*), 7.38 (dq, *J* = 6.7, 6.5, 1.2 Hz, 4H, *j+j'*), 7.22 (dd, *J* = 5.9, 1.8 Hz, 2H, *b*), 2.78 (t, *J* = 7.8 Hz, 4H, *d*), 1.68 (p, *J* = 7.2 Hz, 4H, *e*), 1.26 (m, 48H, *f*), 0.87 (t, *J* = 6.6 Hz, 6H, *g*). ^{13}C NMR (100 MHz, CD_3CN): δ = 158.00 (C_q), 157.98 (C_q), 157.55 (C_q), 155.78 (C_q), 152.61 (CH, *k or k'*), 152.31 (CH, *k or k'*), 151.80 (CH, *c*), 138.52 (CH, *i+i'*), 128.50 (CH, *b, j or j'*), 128.43 (CH, *b, j or j'*), 125.11 (CH, *a+h+h'*), 35.63 (CH_2, *d*), {32.58, 30.79, 30.34, 30.32, 30.29, 30.22, 30.10, 30.02, 29.90, 29.70, 23.33 (CH_2, *e+f*)}, 14.34 (CH_3, *g*). ^{19}F NMR (471 MHz, CD_3CN): δ = -72.43 (d, *J* = 706.6 Hz). UV-Vis (CH_3CN): λ_{max} (ε): 453 nm (1.32×10^4 $mol^{-1}dm^3cm^{-1}$). Phosphorescence (CH_3CN): λ_{ex} = 450 nm, λ_{em} = 613 nm. HRMS (ESI) *m/z* found (calcd): 495.29007 (495.29032, [*M*-2(PF_6)]$^{2+}$), 1135.54224 (1135.54474, [*M*-PF_6]$^+$). Elemental analysis calcd (%) for $C_{60}H_{84}F_{12}N_6P_2Ru$: C 56.29, H 6.61, N 6.56; found: C 57.49, H 7.01, N 6.31.

[Ru(4,4'-($C_{17}H_{35}$)$_2$-bpy)(bpy)$_2$](PF_6)$_2$ (RuC_{17}): from *cis*-[Ru(bpy)$_2$Cl$_2$] (0.75 g, 1.56 mmol) and **4,4'-($C_{17}H_{35}$)$_2$-bpy** (0.98 g, 1.54 mmol). For purification, the crude product was purified via chromatography on silica gel (1st column: acetone/water/brine = 8:4:1, 2nd column: acetone/water/saturated KNO_3 = 100:10:1). The organic solvents were removed under reduced pressure and the red solid was extracted with chloroform (3 x). The combined organic layers were dried over $MgSO_4$ and the solvent was removed under reduced pressure. The red solid was taken up in methanol and subjected to ion exchange column with Amberlite (50 g, pre-soaked with brine and washed 10 x with water and 3 x with methanol). The solvent was removed under reduced pressure and the obtained red solid was redissolved in a mixture of chloroform and brine. The phases were separated, and the aqueous phase was extracted with chloroform (2 x). The combined organic layers were dried over $MgSO_4$ and the solvent was evaporated *in vacuo*. Trituration of the solid in acetone (100 mL) followed by removal of 50 mL of acetone on the rotary evaporator, cooling to room temperature, filtration, and washing with acetone (50 mL) yielded the compound as chloride salt [Ru(4,4'-($C_{17}H_{35}$)$_2$-bpy)(bpy)$_2$](Cl)$_2$·NaCl·3 H_2O. The filtrate was poured into saturated aqueous hexafluorophosphate to yield an orange precipitate

that was filtered and washed with water and collected from the frit with acetone. Removal of the solvent in vacuo yielded **RuC_{17}** as a red solid (yield: 0.32 g, 0.22 mmol, 14%.). ^{1}H NMR (400 MHz, CD_3CN): δ = 8.49 (d, *J* = 8.2 Hz, 4H, *h+h'*), 8.36 (d, *J* = 1.8 Hz, 2H, *a*), 8.04 (ddt, *J* = 8.1, 2.3, 1.5 Hz, 4H, *i+i'*), 7.71 (td, *J* = 5.7, 0.7 Hz, 4H, *k+k'*), 7.54 (d, *J* = 5.8 Hz, 2H, *c*), 7.39 (m, *J* = 7.2, 5.8, 1.3 Hz, 4H, *j+j'*), 7.22 (dd, *J* = 5.8, 1.8 Hz, 2H, *b*), 2.78 (t, *J* = 7.4 Hz, 4H, *d*), 1.68 (p, *J* = 7.2 Hz, 4H, *e*), 1.25 (m, 56H, *f*), 0.86 (t, *J* = 6.7 Hz, 6H, *g*). ^{13}C NMR (100 MHz, CD_3CN): δ = 157.97 (C_q), 157.94 (C_q), 157.51 (C_q), 155.74 (C_q), 152.57 (CH, *k or k'*), 152.36 (CH, *k or k')*, 151.77 (CH, *c*), 138.50 (CH, *i+i'*), 128.48 (CH, *b, j or j'*), 128.42 (CH, *b, j or j'*), 128.39 (CH, *b, j or j'*), 125.09 (CH, *a+h+h'*), 35.60 (CH_2, *d*), {32.56, 30.75, 30.31, 30.29, 30.20, 30.07, 29.99, 29.87, 29.68, 23.31 (CH_2, *e+f*)}, 14.32 (CH_3, *g*). UV-Vis (CH_3CN): λ_{max} (ε): 453 nm (1.69×10^4 $mol^{-1}dm^3cm^{-1}$). Phosphorescence (CH_3CN): λ_{ex} = 450 nm, λ_{em} = 615 nm. HRMS (ESI) *m/z* found (calcd): 523.32126 (523.32168, $[M\text{-}2PF_6]^{2+}$). Elemental analysis calcd (%) for $C_{64}H_{92}F_{12}N_6P_2Ru \cdot 2\ C_3H_6O$: C 57.88, H 7.22, N 5.79; found: C 57.84, H 7.08, N 5.71.

$[Ru(4,4'\text{-}(C_{19}H_{39})_2\text{-}bpy)(bpy)_2](PF_6)_2$ (RuC_{19}): from *cis*-$[Ru(bpy)_2Cl_2]$ (0.10 g, 0.21 mmol) and **$4,4'\text{-}(C_{19}H_{39})_2\text{-}bpy$** (0.20 g, 0.29 mmol). The crude product was purified via chromatography on silica gel (acetone/water/saturated KNO_3 = 100:10:1). After removing all solvents under reduced pressure, the procedure for **RuC_9** was carried out. **RuC_{19}** was finally obtained as a red solid (yield: 36 mg, 0.026 mmol, 8.9%). R_f = 0.2 (SiO_2, acetone/water/saturated KNO_3 100:10:1). ^{1}H NMR (400 MHz, CD_3CN): δ = 8.49 (dd, *J* = 8.2, 1.7 Hz, 4H, *h+h'*), 8.36 (d, *J* = 1.8 Hz, 2H, *a*), 8.04 (tq, *J* = 7.9, 1.8 Hz, 4H, *i+i'*), 7.71 (d, *J* = 5.7, 1.4 Hz, 4H, *k+k'*), 7.54 (d, *J* = 5.8 Hz, 2H, *c*), 7.39 (dq, *J* = 6.1, 5.7, 1.6, 1.2 Hz, 4H, *j+j'*), 7.22 (dd, *J* = 5.8, 1.8 Hz, 2H, *b*), 2.78 (t, *J* = 7.9 Hz, 4H, *d*), 1.68 (p, *J* = 7.0 Hz, 4H, *e*), 1.25 (m, 64H, *f*), 0.87 (t, *J* = 6.5 Hz, 6H, *g*). ^{13}C NMR (100 MHz, CD_3CN): δ = 158.01 (C_q), 157.98 (C_q), 157.55 (C_q), 155.78 (C_q), 152.61 (CH, *k or k'*), 152.40 (CH, *k or k'*), 151.81 (CH, *c*), 138.54 (CH, *i+i'*), 128.52 (CH, *b, j or j'*) 128.45 (CH, *b, j or j'*), 128.42 (CH, *b, j or j'*) 125.12 (CH, *a+h+h'*), 35.64 (CH_2, *d*), {32.59, 30.79, 30.32, 30.23, 30.10, 30.03, 29.90, 29.71, 23.34 (CH_2, *e+f*)}, 14.35 (CH_3, *g*). UV-Vis (CH_3CN): λ_{max} (ε): 453 nm (1.39×10^4 $mol^{-1}dm^3cm^{-1}$). Phosphorescence (CH_3CN): λ_{ex} = 450 nm, λ_{em} = 615 nm. HRMS (ESI) *m/z* found (calcd): 551.35195 (551.35304, $[M\text{-}2(PF_6)]^{2+}$), 1247.66904 (1247.67080, $[M\text{-}PF_6]^+$). Elemental analysis calcd (%) for $C_{68}H_{100}F_{12}N_6P_2Ru^{2+}$: C 58.65, H 7.24, N 6.04; found: C 58.13, H 7.23, N 5.91.

3. Liposome preparation

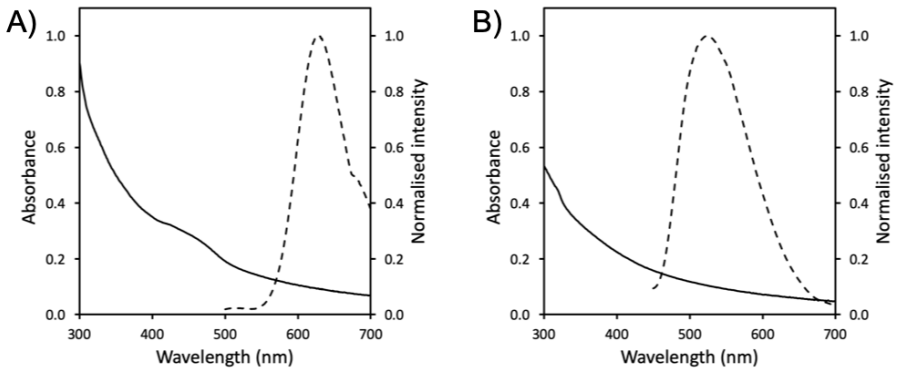

Figure S1. The absorption (solid line) and emission spectrum (dashed line, λ_{exc} = 450 nm for Ru and 380 nm for Re) of A) DSPC:NaDSPE-PEG2K 100:1 liposomes functionalised with **RuC$_{15}$** in 0.1 M NaH_2PO_4 buffer and B) DPPC:NaDSPE-PEG2K 100:1 liposomes functionalised with **ReC$_9$** in 0.1 M NaH_2PO_4 buffer. Experimental conditions: [DPPC or DSPC] = 6.25 mM, [NaDSPE-PEG2K] = 62.5 µM, and [**RuC$_{15}$** or **ReC$_9$**] = 25 µM.

Table S1. Diameter size (d), polydispersity index (PDI), absorption maxima ($\lambda_{abs.}$), and emission maxima (λ_{em}) of liposomes prepared from lipids, NaDSPE-PEG2K, and **RuC$_n$** or **ReC$_n$** in a ratio of 100:1.0:0.4.

	DMPC				DPPC				DSPC			
Sample[a]	**d (nm)**	**PDI**[b]	**λ_{abs}**[c] **(nm)**	**λ_{em} (nm)**	**d (nm)**	**PDI**[b]	**λ_{abs}**[c] **(nm)**	**λ_{em} (nm)**	**d (nm)**	**PDI**[b]	**λ_{abs}**[c] **(nm)**	**λ_{em} (nm)**
RuC$_0$	119	0.09	449	608	147	0.10	420	610	149	0.10	-	608
RuC$_9$	124	0.17	425	635	138	0.11	425	629	164	0.09	456	628
RuC$_{12}$	126	0.15	427	632	143	0.11	427	629	170	0.08	425	625
RuC$_{15}$	134	0.13	425	633	134	0.10	425	627	154	0.10	420	629
RuC$_{17}$	126	0.16	425	634	142	0.11	427	630	157	0.09	-	627
RuC$_{19}$	137	0.15	425	633	143	0.10	424	629	149	0.10	465	625
ReC$_0$	142	0.14	-	553	149	0.09	-	554	153	0.10	-	554
ReC$_9$	143	0.13	-	523	148	0.07	-	525	154	0.09	-	521
ReC$_{12}$	140	0.14	-	520, 552	144	0.07	-	-	163	0.08	-	525
ReC$_{15}$	132	0.12	-	531, 551	148	0.10	-	531, 553	153	0.11	-	526, 553
ReC$_{17}$	143	0.14	-	510, 552	149	0.08	-	554	148	0.07	-	554
ReC$_{19}$	141	0.13	-	554	144	0.08	-	554	152	0.10	-	553

[a] Experimental conditions: [DMPC, DPPC, or DSPC] = 6.25 mM, [NaDSPE-PEG2K] = 62.5 µM, and [**RuC$_n$**] or [**ReC$_n$**] = 25 µM in 0.1 M NaH_2PO_4 buffer. Bulk concentrations [**ReC$_n$**] and [**RuC$_n$**] indicate theoretical concentrations (before extrusion). [b] Liposome size is considered to be uniformly distributed when PDI < 0.2. [c] λ_{abs} could not be determined for rhenium complexes, due to the high levels of lipid scattering at λ_{abs} of the rhenium complexes.

Table S2. Diameter size (d), polydispersity index (PDI), absorption maxima (λ_{abs}), and emission maxima (λ_{em}) of photocatalytic liposomes **C$_n$** prepared from DPPC, NaDSPE-PEG2K, **RuC$_n$**, and **ReC$_n$** in a ratio of 100:1.0:0.4:0.4.

Samples [a]	**d (nm)**[b]	**PDI**[b]	**$\lambda_{em.}$ (nm)**
C_0	130 ± 3	0.066 ± 0.005	601[c], 607[d]
C_9	143 ± 9	0.083 ± 0.001	555[c], 627[c], 632[d]
C_{12}	128 ± 5	0.072 ± 0.016	556[c], 628[c], 630[d]
C_{15}	138 ± 2	0.080 ± 0.012	556[c], 626[c], 628[d]
C_{17}	137 ± 11	0.094 ± 0.006	556[c], 627[c], 627[d]
C_{19}	139 ± 3	0.077 ± 0.003	555[c], 627[c], 628[d]

[a] Experimental conditions: [DPPC] = 6.25 mM, [NaDSPE-PEG2K] = 62.5 µM, [**RuC$_n$**] = 25 µM, and [**ReC$_n$**] = 25 µM in 0.1 M NaH_2PO_4 buffer. Bulk concentrations [**ReC$_n$**] and [**RuC$_n$**] indicate theoretical concentrations (before extrusion). [b] Average over two independent liposome preparations. Liposome size is considered to be uniformly distributed when PDI < 0.2. [c] Excited at 380 nm, [d] excited at 450 nm.

Table S3. Summary of DLS results obtained before and after light irradiation (t_{irr} = 3 h, λ > 455 nm) for photocatalytic liposomes **C$_n$** prepared from DPPC, NaDSPE-PEG2K, **RuC$_n$**, and **ReC$_n$** in a ratio of 100:1.0:0.4:0.4.

	Before irradiation		**After irradiation**	
Sample[a]	**d (nm)**[b]	**PDI**[b]	**d (nm)**[b]	**PDI**[b]
C_0	161 ± 4	0.12 ± 0.01	171 ± 5	0.13 ± 0.01
C_9	157 ± 5	0.11 ± 0.02	172 ± 5	0.18 ± 0.02
C_{12}	150 ± 4	0.12 ± 0.01	164 ± 4	0.16 ± 0.01
C_{15}	119 ± 4	0.11 ± 0.02	131 ± 4	0.17 ± 0.01
C_{17}	158 ± 6	0.10 ± 0.04	165 ± 8	0.11 ± 0.02
C_{19}	155 ± 6	0.10 ± 0.01	162 ± 6	0.14 ± 0.02

[a] Experimental conditions: [DPPC] = 625 µM, [NaDSPE-PEG2K] = 6.25 µM, [**RuC$_n$**] = 2.5 µM, and [**ReC$_n$**] = 2.5 µM in 0.1 M $NaHCO_3$ and 0.1 M NaHAsc solutions at 25 °C. Bulk concentrations [**ReC$_n$**] and [**RuC$_n$**] indicate theoretical concentrations (before extrusion). [b] Average over three independent liposome preparations.

Table S4. Diameter size (d) and polydispersity index (PDI) of photocatalytic liposomes prepared from DPPC, NaDSPE-PEG2K, **RuC_n** and **ReC_n** in a ratio of 100:1.0:0.4:X with X = 0.0, 0.4, and 1.6, which were used for time-resolved spectroscopy measurements.

Sample[a]	**d (nm)**[b]	**PDI**[b]
RuC_9 and 0.0 % ReC_9	146	0.09
RuC_9 and 0.4 % ReC_9	114	0.10
RuC_9 and 1.6 % ReC_9	108	0.18
RuC_{19} and 0.0 % ReC_{19}	136	0.08
RuC_{19} and 0.4 % ReC_{19}	142	0.06
RuC_{19} and 1.6 % ReC_{19}	129	0.09

[a] Experimental conditions: [DPPC] = 6.25 mM, [NaDSPE-PEG2K] = 62.5 µM, [**RuC_n**] = 25 µM, and [**ReC_n**] = 0, 25 or 100 µM in CO_2-saturated 0.1 M NaHAsc aqueous solution. Bulk concentrations [**ReC_n**] and [**RuC_n**] indicate theoretical concentrations (before extrusion). [b] Liposome size is considered to be uniformly distributed when PDI < 0.2.

4. Photocatalysis

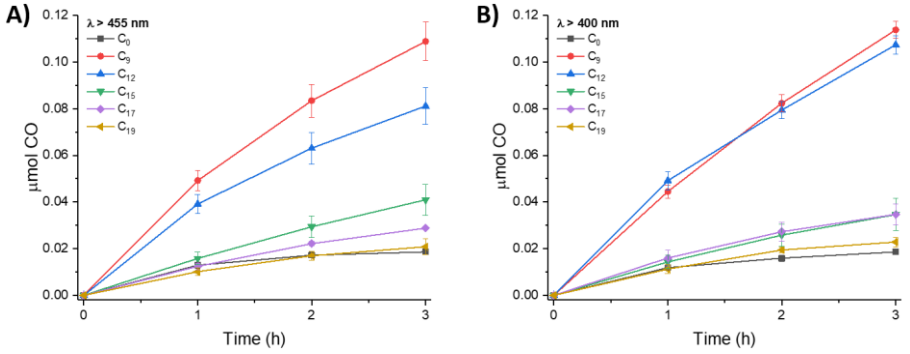

Figure S2. Photocatalytic CO formation after three hours of simulated solar light irradiation (AM 1.5G, 100 mW cm^{-2}) at (A) λ > 455 nm or (B) λ > 400 nm as a function of alkyl chain length for DPPC:NaDSPE-PEG2K 100:1 photocatalytic liposomes **C$_n$** containing **ReC$_n$-RuC$_n$** with the same n. Experimental conditions: [DPPC] = 625 µM, [NaDSPE-PEG2K] = 6.25 µM, [**RuC$_n$**] = 2.5 µM, and [**ReC$_n$**] = 2.5 µM in CO_2-saturated 0.1 M NaH_2PO_4 and 0.1 M NaHAsc aqueous solution (3 mL, pH ≈ 6.3) at 25 °C. Bulk concentrations [**ReC$_n$**] and [**RuC$_n$**] indicate theoretical concentrations (before extrusion). Experiments were performed in triplicates.

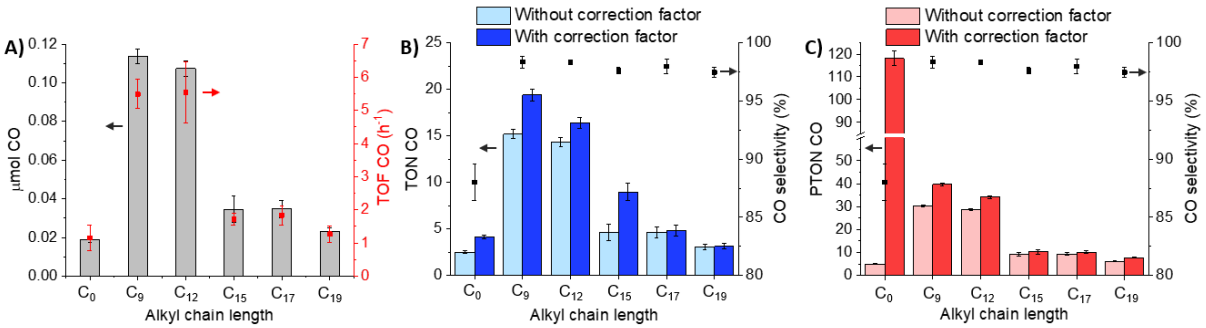

Figure S3. Photocatalytic activity after three hours of simulated solar light irradiation (λ > 400 nm, AM 1.5G, 100 mW cm^{-2}) as a function of alkyl chain length for DPPC:NaDSPE-PEG2K 100:1 photocatalytic liposomes **C$_n$** containing **ReC$_n$-RuC$_n$** with the same n: (A) evolved µmol of CO and uncorrected TOF CO; (B) (light blue) uncorrected and (dark blue) corrected TON CO and CO selectivity; (C) (light red) uncorrected and (dark red) corrected turnover number of CO produced per mol of photosensitiser (PTON CO) and CO selectivity. The TONs and TOFs were obtained after three hours and one hour, respectively. The applied correction (η_{immob}) can be found in Figure 4 and Table S9. Experimental conditions: [DPPC] = 625 µM, [NaDSPE-PEG2K] = 6.25 µM, [**ReC$_n$**] = 2.5 µM and [**RuC$_n$**] = 2.5 µM; CO_2-saturated 0.1 M NaH_2PO_4 and 0.1 M NaHAsc aqueous solution (3 mL, pH ≈ 6.3) at 25 °C. Bulk concentrations [**ReC$_n$**] and [**RuC$_n$**] indicate theoretical concentrations (before extrusion). Experiments were performed in triplicates.

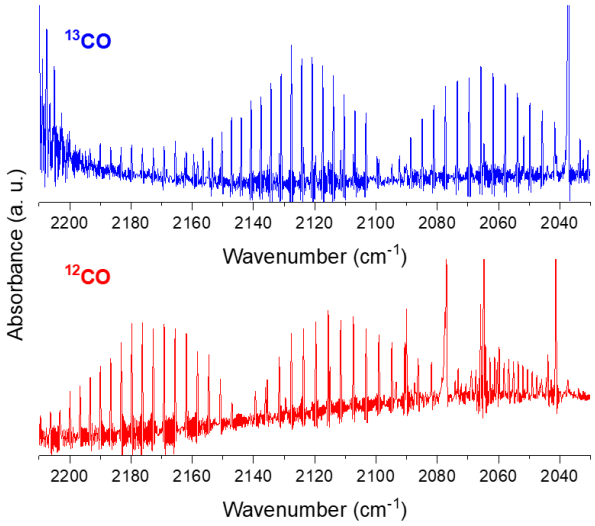

Figure S4. IR absorbance spectra of CO gas obtained from isotopic labelling control experiments using (blue) $^{13}CO_2$ and (red) $^{12}CO_2$ as the headspace gas after three hours of photocatalysis with DPPC:NaDSPE-PEG2K 100:1 photocatalytic liposomes **C$_9$** containing **ReC$_9$** and **RuC$_9$**. Experimental conditions: [DPPC] = 6.25 mM, [NaDSPE-PEG2K] = 62.5 µM, [**RuC$_9$**] = 25 µM, and [**ReC$_9$**] = 25 µM in 0.1 M NaH_2PO_4 and 0.1 M NaHAsc. Bulk concentrations [**ReC$_n$**] and [**RuC$_n$**] indicate theoretical concentrations (before extrusion).

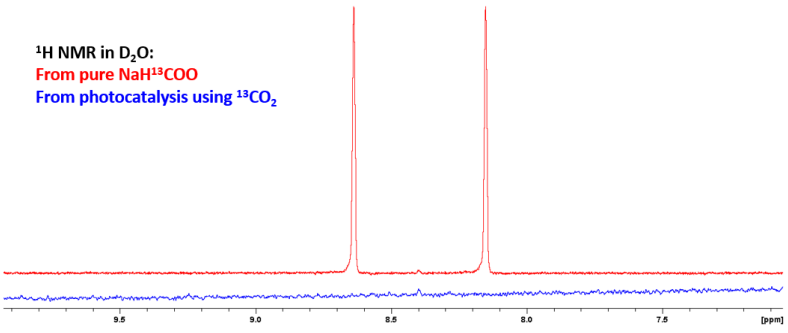

Figure S5. ^{1}H NMR spectra of (red) isotopic labelled sodium formate and (blue) formate obtained from isotopic labelling control experiments using $^{13}CO_2$ as the headspace gas after three hours of photocatalysis using DPPC:NaDSPE-PEG2K 100:1 photocatalytic liposomes **C$_9$** containing **ReC$_9$** and **RuC$_9$**. Experimental conditions: [DPPC] = 6.25 mM, [NaDSPE-PEG2K] = 62.5 µM, [**RuC$_9$**] = 25 µM, and [**ReC$_9$**] = 25 µM in 0.1 M NaH_2PO_4 and 0.1 M NaHAsc. Bulk concentrations [**ReC$_n$**] and [**RuC$_n$**] indicate theoretical concentrations (before extrusion).

Table S5. Summary of photocatalysis results obtained from all alkyl chain lengths in DPPC:NaDSPE-PEG2K 100:1 photocatalytic liposomes **C_n** containing **ReC_n** and **RuC_n** with the same n. All experiments were carried out in CO_2-saturated 0.1 M NaH_2PO_4 and 0.1 M NaHAsc solutions at 25 °C for three hours under visible light (λ > 400 or 455 nm), and in triplicates. In addition to CO and H_2 no other photocatalytic products were detected. TOF and PTOF values were calculated by averaging the obtained values of each hour.

Alkyl chain length	λ (nm)	CO (nmol)	H_2 (nmol)	TON CO	TON H_2	PTON CO	PTON H_2	TOF CO (h^{-1})	TOF H_2 (h^{-1})	PTOF CO (h^{-1})	PTOF H_2 (h^{-1})	CO selectivity (%)
C_0	400	18.6 ± 1.0	2.9 ± 1.2	2.5 ± 0.1	0.4 ± 0.2	5.0 ± 0.1	0.8 ± 0.2	1.2 ± 0.4	0.2 ± 0.1	2.3 ± 0.8	0.3 ± 0.1	88 ± 2
	455	18.6 ± 0.9	0.9 ± 0.1	2.5 ± 0.1	0.1 ± 0.1	5.0 ± 0.1	0.3 ± 0.1	1.2 ± 0.5	< 0.1	2.5 ± 0.9	0.2 ± 0.1	94 ± 1
C_9	400	113.8 ± 3.7	2.5 ± 0.5	15.2 ± 0.5	0.3 ± 0.1	30.3 ± 0.5	0.7 ± 0.1	5.5 ± 0.4	0.1 ± 0.1	11.0 ± 0.9	0.2 ± 0.1	98 ± 1
	455	108.8 ± 8.3	1.1 ± 0.1	14.5 ± 1.1	0.2 ± 0.1	29.0 ± 1.1	0.3 ± 0.1	5.7 ± 0.9	< 0.1	11.3 ± 1.7	0.1 ± 0.1	99 ± 1
C_{12}	400	107.4 ± 3.9	2.0 ± 0.6	14.3 ± 0.5	0.3 ± 0.1	28.6 ± 0.5	0.5 ± 0.1	5.5 ± 0.9	0.1 ± 0.1	11.1 ± 1.8	0.2 ± 0.1	98 ± 1
	455	81.1 ± 7.8	1.4 ± 0.4	10.8 ± 1.0	0.2 ± 0.1	21.6 ± 1.0	0.4 ± 0.1	4.3 ± 0.8	0.1 ± 0.1	8.7 ± 1.6	0.2 ± 0.1	98 ± 1
C_{15}	400	34.6 ± 0.7	0.7 ± 0.2	4.6 ± 0.9	0.1 ± 0.1	9.2 ± 0.9	0.2 ± 0.1	1.7 ± 0.2	< 0.1	3.4 ± 0.4	< 0.1	98 ± 1
	455	40.9 ± 6.6	0.8 ± 0.3	5.5 ± 0.9	0.1 ± 0.1	10.9 ± 0.9	0.2 ± 0.1	2.0 ± 0.1	< 0.1	3.9 ± 0.3	< 0.1	98 ± 1
C_{17}	400	34.7 ± 4.4	1.0 ± 0.3	4.6 ± 0.6	0.1 ± 0.1	9.2 ± 0.6	0.3 ± 0.1	1.8 ± 0.3	< 0.1	3.7 ± 0.6	< 0.1	98 ± 1
	455	28.8 ± 0.3	0.5 ± 0.1	3.8 ± 0.1	< 0.1	7.7 ± 0.1	< 0.1	1.5 ± 0.2	< 0.1	2.9 ± 0.4	< 0.1	97 ± 2
C_{19}	400	22.8 ± 2.0	0.5 ± 0.1	3.0 ± 0.3	< 0.1	6.1 ± 0.3	0.1 ± 0.1	1.3 ± 0.2	< 0.1	2.5 ± 0.5	< 0.1	97 ± 1
	455	20.8 ± 3.3	0.5 ± 0.1	2.8 ± 0.4	< 0.1	5.5 ± 0.4	0.1 ± 0.1	1.1 ± 0.2	< 0.1	2.3 ± 0.4	< 0.1	98 ± 1

Table S6. Summary of photocatalysis results for CO gas obtained from all alkyl chain lengths in DPPC:NaDSPE-PEG2K 100:1 photocatalytic liposomes **C_n** containing **ReC_n** and **RuC_n** with the same n before and after applying η_{immob} as correction factor (Table S9). Non-corrected data is also shown in Table S5.

Alkyl chain length	λ (nm)	TON CO	^{corr}TON CO	PTON CO	^{corr}PTON CO	TOF CO (h^{-1})	^{corr}TOF CO (h^{-1})	PTOF CO (h^{-1})	^{corr}PTOF CO (h^{-1})
C_0	400	2.5 ± 0.1	4.1 ± 0.2	5.0 ± 0.1	118.1 ± 3.2	1.2 ± 0.4	1.9 ± 0.6	2.3 ± 0.8	55.0 ± 18.4
	455	2.5 ± 0.1	4.1 ± 0.2	5.0 ± 0.1	118.2 ± 3.0	1.2 ± 0.5	2.1 ± 0.8	2.5 ± 0.9	68.3 ± 21.6
C_9	400	15.2 ± 0.5	19.4 ± 0.6	30.3 ± 0.5	39.7 ± 0.7	5.5 ± 0.4	7.0 ± 0.6	11.0 ± 0.9	14.4 ± 1.1
	455	14.5 ± 1.1	18.6 ± 1.4	29.0 ± 1.1	38.0 ± 1.4	5.7 ± 0.9	7.2 ± 1.1	11.3 ± 1.7	14.8 ± 2.3
C_{12}	400	14.3 ± 0.5	16.4 ± 0.6	28.6 ± 0.5	34.2 ± 0.6	5.5 ± 0.9	6.3 ± 1.0	11.1 ± 1.8	13.2 ± 2.2
	455	10.8 ± 1.0	12.4 ± 1.2	21.6 ± 1.0	25.8 ± 1.2	4.3 ± 0.8	5.0 ± 0.9	8.7 ± 1.6	10.4 ± 1.9
C_{15}	400	4.6 ± 0.9	6.3 ± 1.3	9.2 ± 0.9	10.9 ± 1.1	1.7 ± 0.2	2.4 ± 0.3	3.4 ± 0.4	4.1 ± 0.4
	455	5.5 ± 0.9	7.5 ± 1.2	10.9 ± 0.9	12.9 ± 1.0	2.0 ± 0.1	2.7 ± 0.2	3.9 ± 0.3	4.6 ± 0.3
C_{17}	400	4.6 ± 0.6	4.8 ± 0.6	9.2 ± 0.6	10.2 ± 0.7	1.8 ± 0.3	1.9 ± 0.3	3.7 ± 0.6	4.0 ± 0.7
	455	3.8 ± 0.1	4.0 ± 0.1	7.7 ± 0.1	8.5 ± 0.1	1.5 ± 0.2	1.5 ± 0.2	2.9 ± 0.4	3.2 ± 0.4
C_{19}	400	3.0 ± 0.3	3.1 ± 0.3	6.1 ± 0.3	7.8 ± 0.3	1.3 ± 0.2	1.3 ± 0.3	2.5 ± 0.5	3.3 ± 0.6
	455	2.8 ± 0.4	2.9 ± 0.5	5.5 ± 0.4	7.1 ± 0.6	1.1 ± 0.2	1.2 ± 0.2	2.3 ± 0.4	2.9 ± 0.6

Table S7. Summary of photocatalysis experiments obtained from all alkyl chain lengths in DPPC:NaDSPE-PEG2K 100:1 photocatalytic liposomes **C_n**. All experiments were conducted in CO_2- or N_2- saturated 0.1 M NaH_2PO_4 and 0.1 M NaHAsc buffer solutions for three hours at 25 °C under visible light (λ > 455 nm) and in duplicates, except for the first row in C_9 system whose experiments were performed as triplicates. Symbols "✓" and "-" stand for "included" and "not included" respectively, and "n. d." stands for "not detected".

Alkyl chain length	Components				Gaseous products after three-hour experiments				
	Catalyst	Photosensitiser	Sodium ascorbate	CO_2	CO (nmol)	H_2 (nmol)	TON CO	TON H_2	CO selectivity (%)
C_0	✓	-	✓	✓	n. d.	n. d.	-	-	-
	-	✓	✓	✓	0.1 ± 0.1	0.1 ± 0.1	-	-	-
C_9	✓	✓	✓	✓	108.9 ± 8.3	1.1 ± 0.1	14.5 ± 1.1	0.2 ± 0.1	99 ± 1
	✓	✓	✓	✓[a]	n. d.	n. d.	-	-	-
	✓	✓	-	✓	n. d.	n. d.	-	-	-
	✓	✓	✓	-[b]	n. d.	n. d.	-	-	-
	✓	-	✓	✓	n. d.	n. d.	-	-	-
	-	✓	✓	✓	0.2 ± 0.1	n. d.	-	-	-
C_{12}	✓	-	✓	✓	0.2 ± 0.1	n. d.	-	-	-
	-	✓	✓	✓	n. d.	n. d.	-	-	-
C_{15}	✓	-	✓	✓	n. d.	n. d.	-	-	-
	-	✓	✓	✓	0.3 ± 0.1	n. d.	-	-	-
C_{17}	✓	-	✓	✓	0.3 ± 0.1	0.3 ± 0.1	-	-	-
	-	✓	✓	✓	n. d.	n. d.	-	-	-
C_{19}	✓	-	✓	✓	0.1 ± 0.1	n. d.	-	-	-
	-	✓	✓	✓	0.3 ± 0.1	n. d.	-	-	-

[a] Experiments were carried out in the dark. [b] Experiments were carried out in N_2-saturated solutions.

5. Electrochemistry

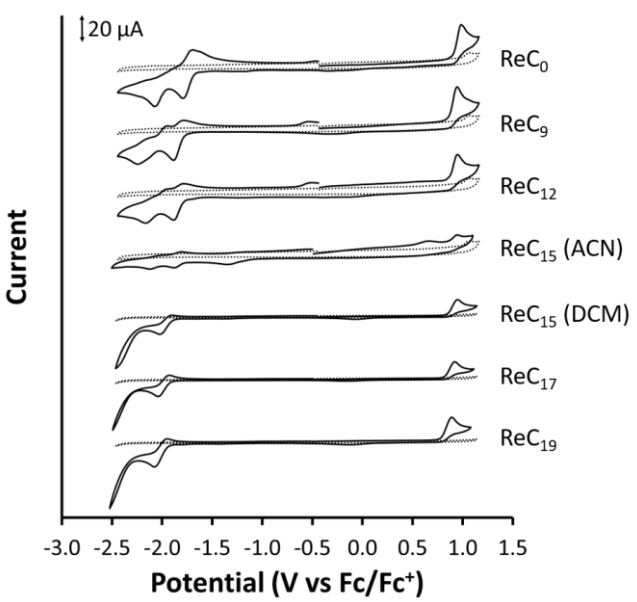

Figure S6. Cyclic voltammograms of solutions of **ReC$_n$** (1 mM) in degassed acetonitrile (**ReC$_0$**, **ReC$_9$**, **ReC$_{12}$**, and **ReC$_{15}$**) or degassed dichloromethane (**ReC$_{15}$**, **ReC$_{17}$**, and **ReC$_{19}$**) with 0.1 M Bu_4NPF_6 electrolyte, measured at 25 °C. The voltammograms were obtained at a scanning rate of 100 mV s^{-1} with a glassy carbon working electrode, Ag/AgCl reference electrode, and a Pt wire auxiliary electrode.

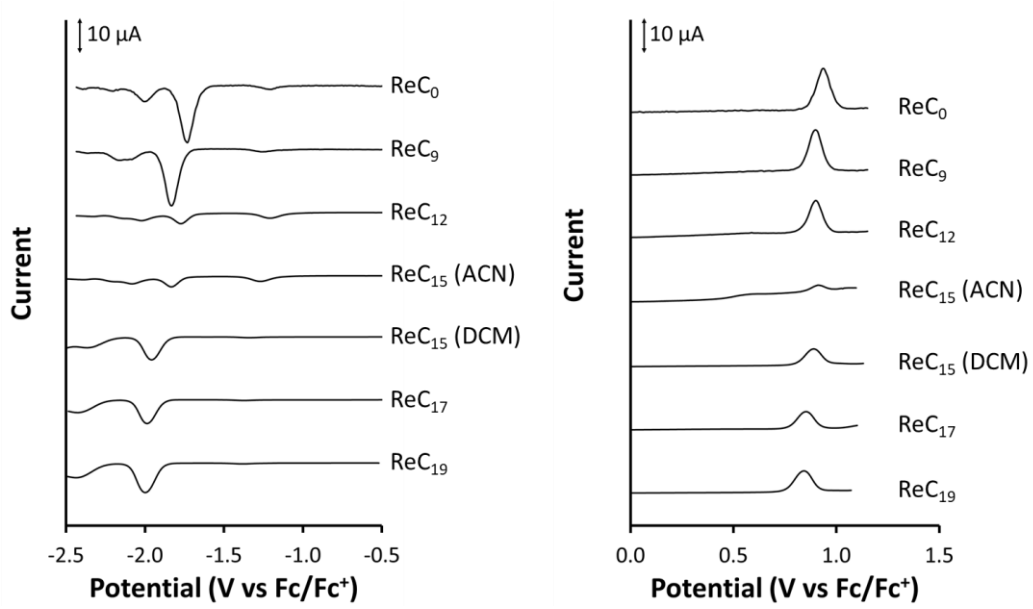

Figure S7. Differential pulse voltammograms of solutions of **ReC$_n$** (1 mM) in degassed acetonitrile (**ReC$_0$**, **ReC$_9$**, **ReC$_{12}$**, and **ReC$_{15}$**) or degassed dichloromethane (**ReC$_{15}$**, **ReC$_{17}$**, and **ReC$_{19}$**) with 0.1 M Bu_4NPF_6 electrolyte, measured at 25 °C. The voltammograms were obtained at a scanning rate of 50 mV s^{-1} with a glassy carbon working electrode, Ag/AgCl reference electrode, and a Pt wire auxiliary electrode.

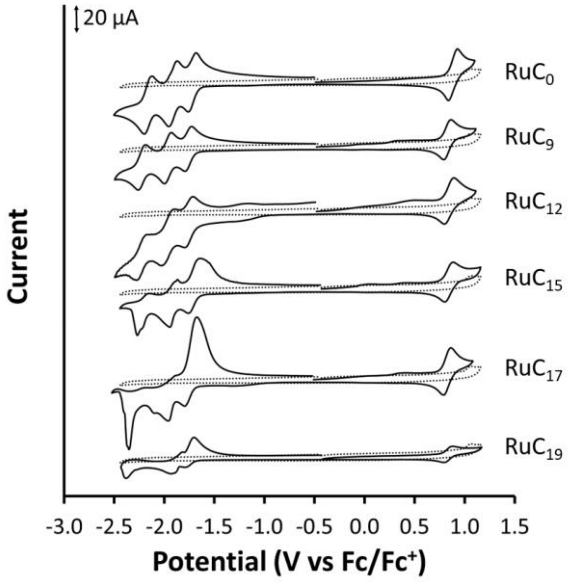

Figure S8. Cyclic voltammograms of solutions of **RuC$_n$** (1 mM) in degassed acetonitrile with 0.1 M Bu_4NPF_6 electrolyte, measured at 25 °C. The voltammograms were obtained at a scanning rate of 100 mV s^{-1} with a glassy carbon working electrode, Ag/AgCl reference electrode, and a Pt wire auxiliary electrode.

Table S8. Redox potentials of **RuC$_n$** and **ReC$_n$** complexes.[a]

Metal complex	$E_{1/2}$ (oxdn) in V *vs.* Fc^+/Fc	$E_{1/2}$ (redn) in V *vs.* Fc^+/Fc
RuC_0	0.88	-1.72, -1.92, -2.16
RuC_9	0.83	-1.76, -1.97, -2.22
RuC_{12}	0.84	-1.70, -1.91, -2.20
RuC_{15}	0.84	-1.70, -1.91, -2.20
RuC_{17}	0.80	-1.76, -1.92, -2.26
RuC_{19}	0.83	-1.74, -1.87, -2.35
ReC_0	0.94	-1.73, -2.00
ReC_9	0.90	-1.83, -2.15
ReC_{12}	0.90	-1.83, -2.12
ReC_{15}	0.91[b]	-1.83[b], -2.08[b]
	0.89[c]	-1.96[c], -2.37[c]
ReC_{17}	0.85[c]	-1.99[c], -2.43[c]
ReC_{19}	0.84[c]	-2.00[c], -2.44[c]

[a] These values were obtained at 25 °C in degassed acetonitrile solutions containing 0.1 M tetrabutylammonium hexafluorophosphate and 1 mM metal complex. [b] **ReC$_{15}$** was partially soluble in acetonitrile. [c] These values were measured in degassed dichloromethane.

6. Liposome immobilisation efficiency

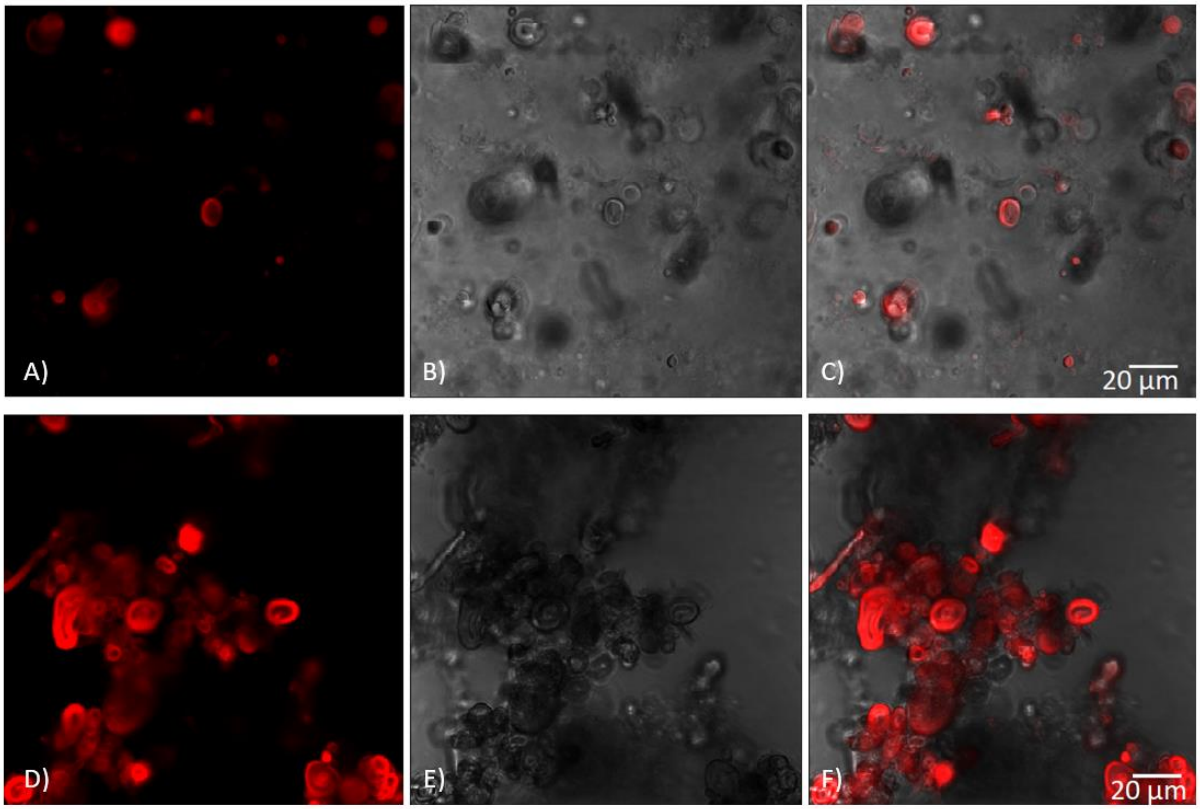

Figure S9. Confocal microscopy of DPPC (A, B, C) and DMPC (D, E, F) giant vesicles containing 2% **RuC_{12}** in 0.1 M NaH_2PO_4 buffer (pH = 7.7). Figures S9A and S9D are fluorescence images, Figures S9B and S9E are transmission images, and Figures S9C and S9F are overlay images. Images were taken with a Nikon Ti2 microscope at 80x total zoom, 488 nm excitation, and 640 – 680 nm emission.

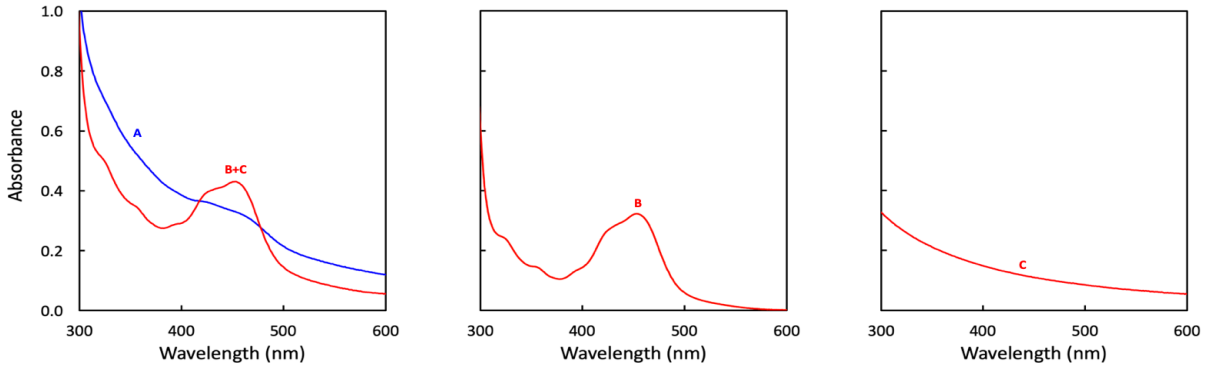

Figure S10. UV-Vis absorption spectra of A) DSPC:NaDSPE-PEG2K 100:1 liposomes functionalised with **RuC_{12}** in 0.1 M NaH_2PO_4 buffer (blue line), B) **RuC_{12}** in acetonitrile (no liposomes), C) DSPC:NaDSPE-PEG2K 100:1 liposomes (without **RuC_{12}**) in 0.1 M NaH_2PO_4 buffer. Red curve in A shows the addition of the absorption spectra of B and C; it obviously does not superpose to the absorption spectrum of the Ru-functionalised liposomes (blue line), illustrating the limits of UV-vis spectroscopy for quantifying the **RuC_{12}** concentration in liposomes. Experimental conditions: [DSPC] = 6.25 mM, [NaDSPE-PEG2K] = 62.5 µM, and [RuC_{12}] = 25 µM.

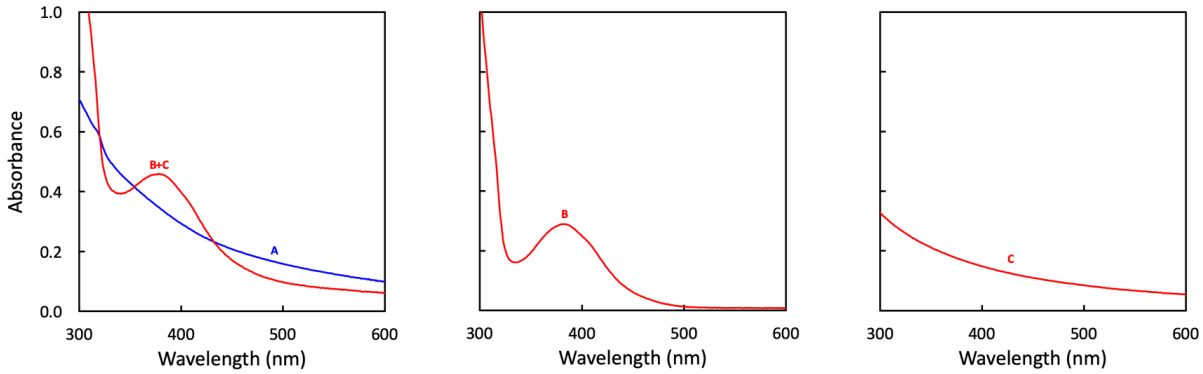

Figure S11. UV-Vis absorption spectra of A) DSPC:NaDSPE-PEG2K 100:1 liposomes functionalised with **ReC$_{12}$** in 0.1 M NaH_2PO_4 buffer, B) **ReC$_{12}$** in chloroform (no liposomes), C) DSPC:NaDSPE-PEG2K 100:1 liposomes (without **ReC$_{12}$**) in 0.1 M NaH_2PO_4 buffer. Red curve in A shows the addition of the absorption spectra of B and C; it obviously does not superpose with the absorption spectrum of the Re-functionalised liposomes (blue line), illustrating the limits of UV-vis spectroscopy for quantifying the **ReC$_{12}$** concentration in liposomes. Experimental conditions: [DSPC] = 6.25 mM, [NaDSPE-PEG2K] = 62.5 µM, and [ReC_{12}] = 25 µM.

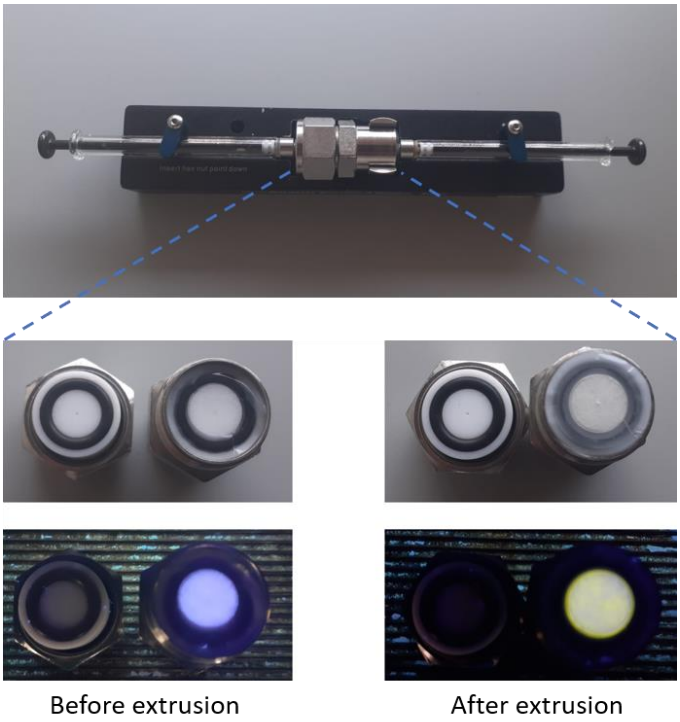

Figure S12. The Avanti Polar Lipids mini-extruder used to prepare liposomes (in this case DPPC:PEG2K:**RuC$_9$**:**ReC$_9$** in a ratio 100:1.0:0.4:0.4) and the internal membrane supports including the filter supports and the polycarbonate membrane (0.2 µm) before and after extrusion. A deposit was observed on the filter after extrusion, which coloured brightly yellow under UV light (λ = 366 nm), which indicated that some **ReC$_9$** (λ_{abs} = 380 nm and λ_{em} = 582 nm in chloroform) was present on the filter.

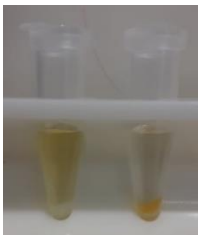

Figure S13. Solutions of **RuC$_0$-ReC$_0$** liposomes (left) and **RuC$_9$-ReC$_9$** liposomes (right) after ultracentrifugation.

Table S9. Immobilisation efficiencies, determined by ICP-MS, for photocatalytic liposomes **C$_n$** prepared from DPPC, NaDSPE-PEG2K, **RuC$_n$**, and **ReC$_n$** (100:1.0:0.4:0.4).[a]

Metal complex	η_{extr}[b]	η_{encap}[b]	η_{immob}[b]
RuC_0	94.9 ± 5.1%	4.2 ± 4.2%	3.8 ± 3.8%
RuC_9	80.3 ± 1.1%	95.0 ± 0.8%	76.3 ± 1.7%
RuC_{12}	86.4 ± 0.2%	97.0 ± 0.5%	83.8 ± 0.3%
RuC_{15}	85.2 ± 6.3%	99.6 ± 0.3%	84.9 ± 6.0%
RuC_{17}	91.2 ± 5.1%	99.5 ± 0.2%	90.7 ± 5.2%
RuC_{19}	78.6 ± 2.7%	99.2 ± 0.1%	78.0 ± 2.6%
ReC_0	95.1 ± 4.9%	62.0 ± 5.5%	59.3 ± 8.2%
ReC_9	80.2 ± 10.9%	97.5 ± 0.8%	78.1 ± 10.0%
ReC_{12}	86.1 ± 14.0%	97.4 ± 0.6%	83.7 ± 13.1%
ReC_{15}	75.2 ± 22.3%	97.2 ± 0.6%	73.2 ± 22.2%
ReC_{17}	96.2 ± 3.8%	98.4 ± 1.0%	94.7 ± 4.7%
ReC_{19}	99.3 ± 0.7%	96.9 ± 0.4%	96.2 ± 1.1%

[a] Experimental conditions: [DPPC] = 6.25 mM, [NaDSPE-PEG2K] = 62.5 µM, [**RuC$_n$**] = 25 µM, and [**ReC$_n$**] = 25 µM in 0.1 M NaH_2PO_4 buffer. Bulk concentrations [**ReC$_n$**] and [**RuC$_n$**] indicate theoretical concentrations (before extrusion). [b] The errors are based on two independent liposome preparations.

7. Transient absorption (TA) spectroscopy

7.1 Supplementary figures

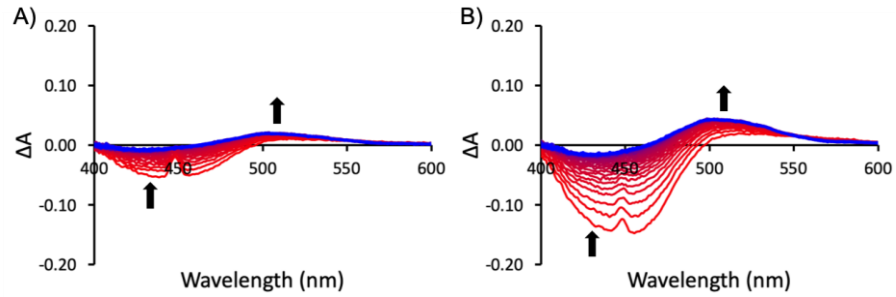

Figure S14. Time-resolved absorption spectroscopy data after laser excitation (λ_{exc} = 450 nm, 3.5 mJ per pulse) on a 2 µs timescale (timestep = 0.04 µs) for DPPC-NaDSPE-PEG2K liposome systems **C$_n$** consisting of A) **RuC$_9$** and 0.0% **ReC$_9$** and B) **RuC$_{19}$** and 0.0% **ReC$_{19}$**. Experimental conditions: [DPPC] = 6.25 mM, [NaDSPE-PEG2K] = 62.5 µM, and [**RuC$_n$**] = 25 µM in CO_2-saturated 0.1 M NaHAsc aqueous solution. Bulk concentration [**RuC$_n$**] indicates theoretical concentration (before extrusion). The observed artefact in the data at 450 nm is due to the scattering of laser light.

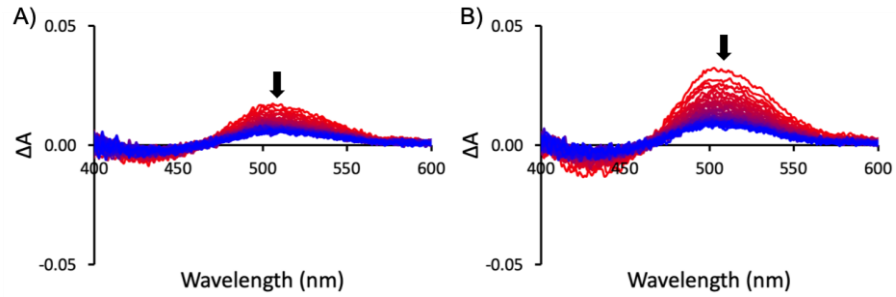

Figure S15. Time-resolved absorption spectroscopy data after laser excitation (λ_{exc} = 450 nm, 3.5 mJ per pulse) on a 2 ms timescale (timestep = 0.04 ms) for DPPC-NaDSPE-PEG2K liposome systems **C$_n$** consisting of A) **RuC$_9$** and 0.0% **ReC$_9$** and B) **RuC$_{19}$** and 0.0% **ReC$_{19}$**. Experimental conditions: [DPPC] = 6.25 mM, [NaDSPE-PEG2K] = 62.5 µM, and [**RuC$_n$**] = 25 µM in CO_2-saturated 0.1 M NaHAsc aqueous solution. Bulk concentration [**RuC$_n$**] indicates theoretical concentration (before extrusion).

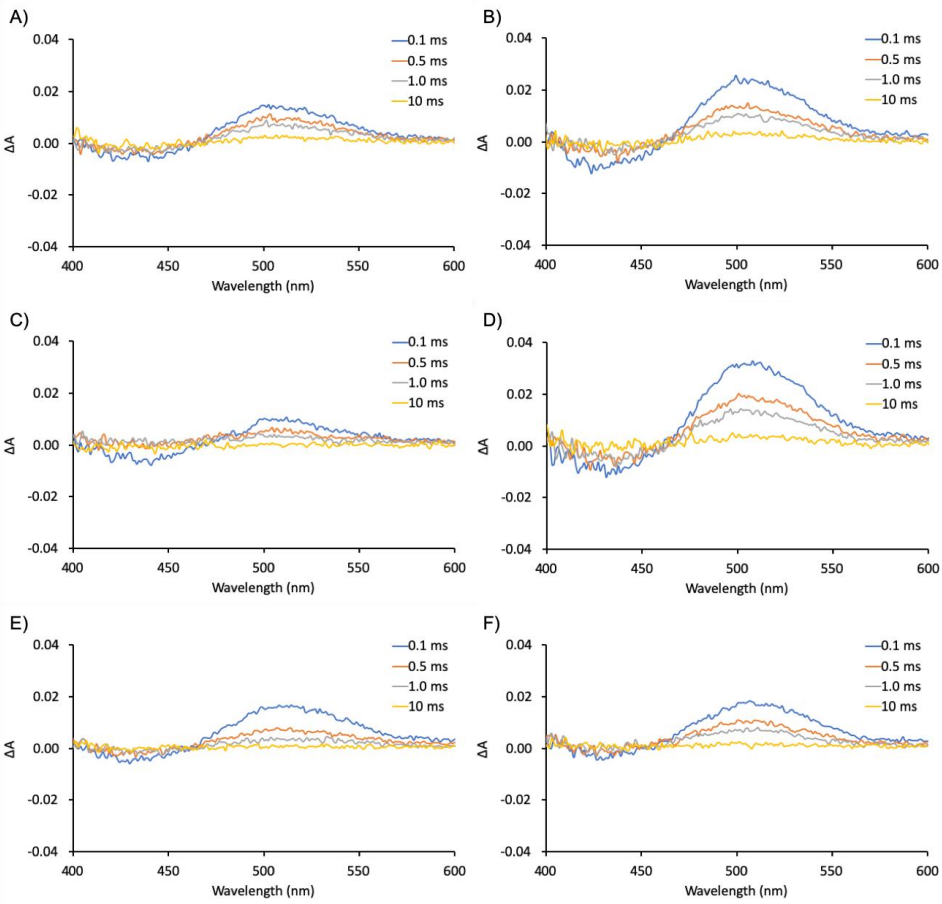

Figure S16. Time-resolved absorption spectroscopy data after laser excitation (λ_{exc} = 450 nm, 3.5 mJ per pulse) on a 10 ms timescale (timestep = 0.1 ms) for DPPC-NaDSPE-PEG2K liposome systems **C$_n$** consisting of A) **RuC$_9$** and 0.0% **ReC$_9$**, B) **RuC$_{19}$** and 0.0% **ReC$_{19}$**, C) **RuC$_9$** and 0.4% **ReC$_9$**, D) **RuC$_{19}$** and 0.4% **ReC$_{19}$**, E) **RuC$_9$** and 1.6% **ReC$_9$**, and F) **RuC$_{19}$** and 1.6% **ReC$_{19}$**. Experimental conditions: [DPPC] = 6.25 mM, [NaDSPE-PEG2K] = 62.5 µM, [**RuC$_n$**] = 25 µM, and [**ReC$_n$**] = 0, 25 or 100 µM in CO_2-saturated 0.1 M NaHAsc aqueous solution. Bulk concentrations [**ReC$_n$**] and [**RuC$_n$**] indicate theoretical concentrations (before extrusion).

7.2 Kinetic model

In the absence of quencher **ReC$_n$**, the rate equation for **RuC$_n^-$** is a combination of the formation of **RuC$_n^-$** due to reductive quenching of **RuC$_n^*$** by $HAsc^-$ and the decay of **RuC$_n^-$** due to the second-order charge recombination of **RuC$_n^-$** and $HAsc^\bullet$ (Equation S5). The disappearance of **RuC$_n^*$** is very fast (µs) in comparison to the disappearance of **RuC$_n^-$** (ms). The TA spectroscopy measurements were performed in the ms timescale (10 ms with a timestep of 0.1 ms) and thus the rate equation for **RuC$_n^-$** simplifies to Equation S6. Assuming that $[\mathbf{RuC_n^-}]_0$ equals $[HAsc^\bullet]_0$ leads to a standard second order rate law (Equation S7) with its solution (Equation S8), which can be rewritten to Equation 4.

$$\frac{d[\mathrm{Ru}C_n^-]}{dt} = k_{\mathrm{RQ}}[\mathrm{Ru}C_n^*][HAsc^-] - k_{\mathrm{CR}}[\mathrm{Ru}C_n^-][HAsc^\bullet] \qquad \text{Equation S5}$$

$$\frac{d[\mathrm{Ru}C_n^-]}{dt} = -k_{\mathrm{CR}}[\mathrm{Ru}C_n^-][HAsc^\bullet] \qquad \text{Equation S6}$$

$$\frac{d[\mathrm{Ru}C_n^-]}{dt} = -k_{\mathrm{CR}}[\mathrm{Ru}C_n^-]^2 \qquad \text{Equation S7}$$

$$\frac{1}{[\mathrm{Ru}C_n^-]} = \frac{1}{[\mathrm{Ru}C_n^-]_0} + k_{\mathrm{CR}}t \qquad \text{Equation S8}$$

In the presence of quencher **ReC$_n$**, the rate equation for **RuC$_n^-$** is a combination of the decay of **RuC$_n^-$** due to second-order charge recombination of **RuC$_n^-$** and HAsc$^\bullet$ and due to first-order quenching by **ReC$_n$** (Equation S9). Equation S9 can be solved according to Limburg et al.[8] to give Equation 6 in the main text.

$$\frac{d[\mathrm{Ru}C_n^-]}{dt} = -k_{\mathrm{CR}}[\mathrm{Ru}C_n^-][HAsc^\bullet] - k_{\mathrm{Q}}[ReC_n] \qquad \text{Equation S9}$$

7.3 Data fitting

The average absorbance between 490 – 540 nm was fitted using Equation S10 and S11, which is derived from Equation 5 in the main text using the Lambert-Beer law. At these wavelengths the concentration and absorption of **RuC$_n^-$** are strictly proportional to the optical pathlength (l = 1 cm) and the molar extinction coefficient ($\varepsilon_{505\mathrm{nm}}$ = 1.2 x 10^4 $M^{-1}cm^{-1}$ for $[Ru(bpy)_3]^+$ in acetonitrile[9] was used).

$$A(t) = \frac{A_0}{1 + k' A_0 t} + A_\infty \qquad \text{Equation S10}$$

$$k' = \frac{k_{CR}}{\varepsilon_{505}\, l} \qquad \text{Equation S11}$$

Table S10. Fitting parameters used to fit the data in Figure 5 using Equation S10.

Sample	A_0	$k'\varepsilon_{505}c_0 l$ (μs^{-1})	A_∞ (10^3)
RuC$_9$ and 0.0 % **ReC$_9$**	0.011 ± 0.003	131 ± 7	1.26 ± 0.07
RuC$_9$ and 0.4 % **ReC$_9$**	0.012 ± 0.003	651 ± 103	0.60 ± 0.09
RuC$_9$ and 1.6 % **ReC$_9$**	0.022	334 ± 12	-0.20 ± 0.04
RuC$_{19}$ and 0.0 % **ReC$_{19}$**	0.019 ± 0.004	100 ± 4	1.79 ± 0.07
RuC$_{19}$ and 0.4 % **ReC$_{19}$**	0.0286 ± 0.0004	73 ± 2	1.50 ± 0.06
RuC$_{19}$ and 1.6 % **ReC$_{19}$**	0.0160 ± 0.0003	149 ± 5	0.54 ± 0.05

8. Fluorescence correlation spectroscopy

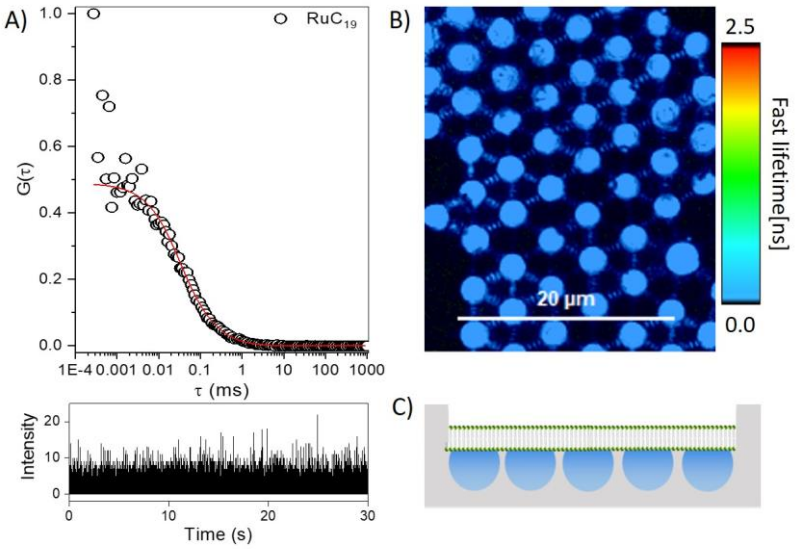

Figure S17. A) top ACF and bottom time trace for diffusion of **RuC_{19}** in acetonitrile. The diffusion coefficient in solution was measured by fitting this curve to a three-dimensional model with D equals 199 ± 149 $\mu m^2 s^{-1}$ with an α value of 0.99 ± 0.08. B) Fluorescence lifetime image of MSLBs comprised of DPPC:NaDSPE-PEG2K in a ratio of 100:1. The membrane is labelled with 10 nM DOPE-ATTO 655 and the image shows the fluorescence from the ATTO probe above the pores of the arrays confirming that the bilayer has formed. C) Schematic illustration of aqueous filled microcavity supported lipid bilayer. Note we have included the organic probe to image the bilayer, because the much lower quantum yield of the Ru compound makes it difficult to see it in fluorescence lifetime imaging above the pores against background/scatter from the substrate.

9. Single crystal X-ray crystallography of 4,4'-$(C_{17}H_{35})_2$-bpy

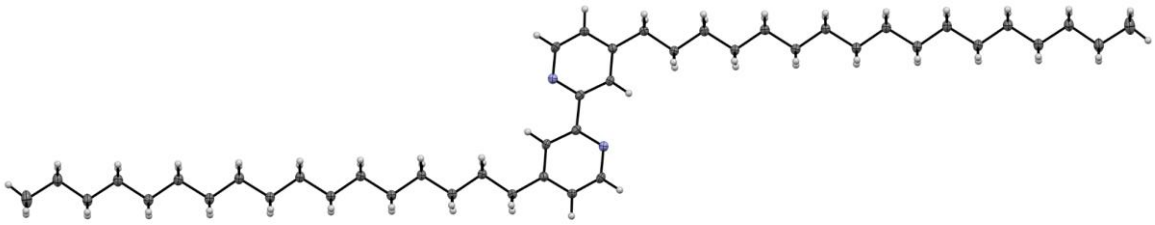

Figure S18. Displacement ellipsoid plots (50% probability level) of **4,4'-$(C_{17}H_{35})_2$-bpy** at 110(2) K.

Colourless single crystals of **4,4'-$(C_{17}H_{35})_2$-bpy** were obtained by evaporation of the solvent $CDCl_3$ at room temperature. Deposition numbers 2062217 (https://www.ccdc.cam.ac.uk/services/structures?id=doi:10.1002/chem.202102989) (for **4,4'-$(C_{17}H_{35})_2$-bpy**) contain(s) the supplementary crystallographic data for this paper. These data are provided free of charge by the joint Cambridge Crystallographic Data Centre and Fachinformationszentrum Karlsruhe (http://www.ccdc.cam.ac.uk/structures).

All reflection intensities were measured at 110(2) K using a SuperNova diffractometer (equipped with Atlas detector) with Cu Kα radiation (λ = 1.54178 Å) under the program CrysAlisPRO (Version CrysAlisPro 1.171.39.29c, Rigaku OD, 2017, Oxford Diffraction / Agilent Technologies UK Ltd, Yarnton, England). The same program was used to refine the cell dimensions and for data reduction. The structure was solved with the program SHELXS-2018/3[10] and was refined on F^2 with SHELXL-2018/3[10]. Analytical numeric absorption correction using a multifaceted crystal model was applied using CrysAlisPro. The temperature of the data collection was controlled using the system Cryojet (manufactured by Oxford Instruments). The H atoms were placed at calculated positions using the instruction AFIX 23, AFIX 43 or AFIX 137 with isotropic displacement parameters having values 1.2 or 1.5 *U*eq of the attached C atoms.

The structure is ordered. The crystal that was mounted on the diffractometer was a composite of two crystals stuck together (most crystals were significantly twinned). The two crystals are related by a rotation of *ca.* 3.74° around the b direction. The refinement was carried out using the HKLF5 instruction, and the BASF scale factor refines to 0.135(2).

Table S11. Experimental details.

	xs2388a
Crystal data	
Chemical formula	$C_{44}H_{76}N_2$
M_r	633.06
Crystal system, space group	Triclinic, *P*-1
Temperature (K)	110
a, *b*, *c* (Å)	6.4931 (4), 7.0030 (4), 21.8388 (11)
α, β, γ (°)	80.932 (4), 86.310 (5), 86.295 (4)
V (Å^3)	977.10 (10)
Z	1
Radiation type	Cu *K*α
m (mm^{-1})	0.45
Crystal size (mm)	0.29 × 0.09 × 0.02
Data collection	
Diffractometer	SuperNova, Dual, Cu at zero, Atlas
Absorption correction	Analytical CrysAlis PRO 1.171.39.29c (Rigaku OD, 2017) Analytical numeric absorption correction using a multifaceted crystal model based on expressions derived by R.C. Clark & J.S. Reid.[11] Empirical absorption correction using spherical harmonics, implemented in SCALE3 ABSPACK (An Oxford Diffraction Program (1.0.4, gui:1.0.3) © 2005 Oxford Diffraction Ltd.) scaling algorithm.
T_{min}, T_{max}	0.929, 0.991
No. of measured, independent and observed [$I > 2s(I)$] reflections	11246, 3934, 1773
R_{int}	0.030
$(\sin \theta/l)_{max}$ (Å^{-1})	0.598
Refinement	
$R[F^2 > 2s(F^2)]$, $wR(F^2)$, *S*	0.036, 0.093, 0.71
No. of reflections	3934
No. of parameters	210
H-atom treatment	H-atom parameters constrained
$\Delta\rho_{max}$, $\Delta\rho_{min}$ (e Å^{-3})	0.15, -0.18

Computer programs: CrysAlis PRO 1.171.39.29c (Rigaku OD, 2017), SHELXS2018/3[10], SHELXL2018/3[10], SHELXTL v6.10[12].

10. NMR of the synthesised compounds

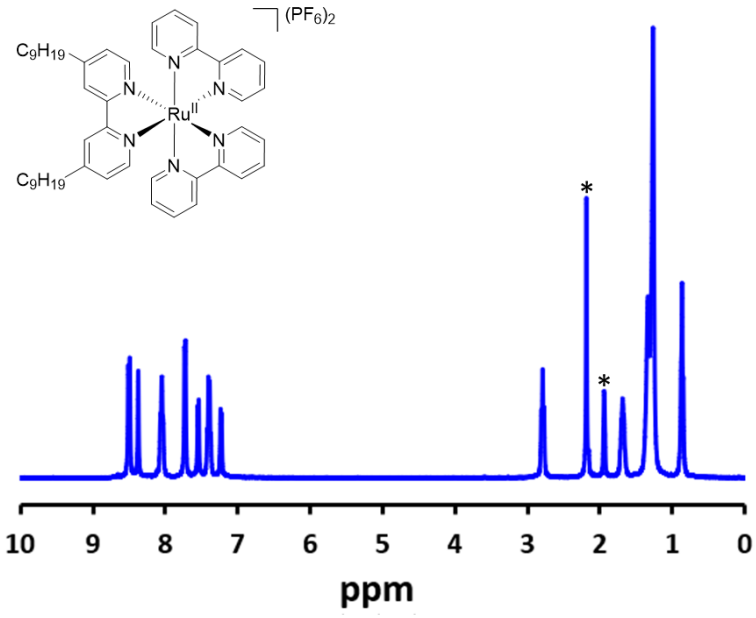

Figure S19. ^{1}H-NMR of **RuC$_9$** in CD_3CN. Solvent peaks are indicated with *.

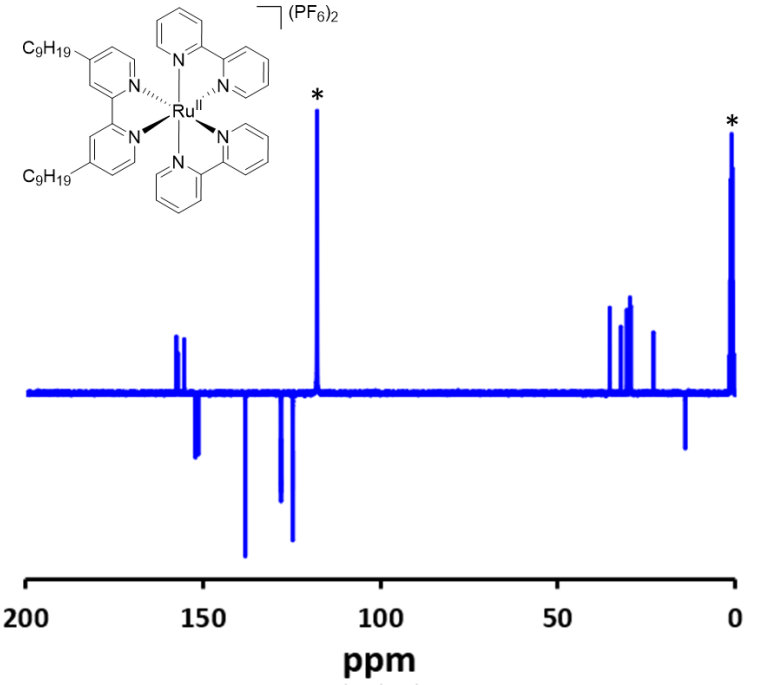

Figure S20. ^{13}C-NMR of **RuC$_9$** in CD_3CN. Solvent peaks are indicated with *.

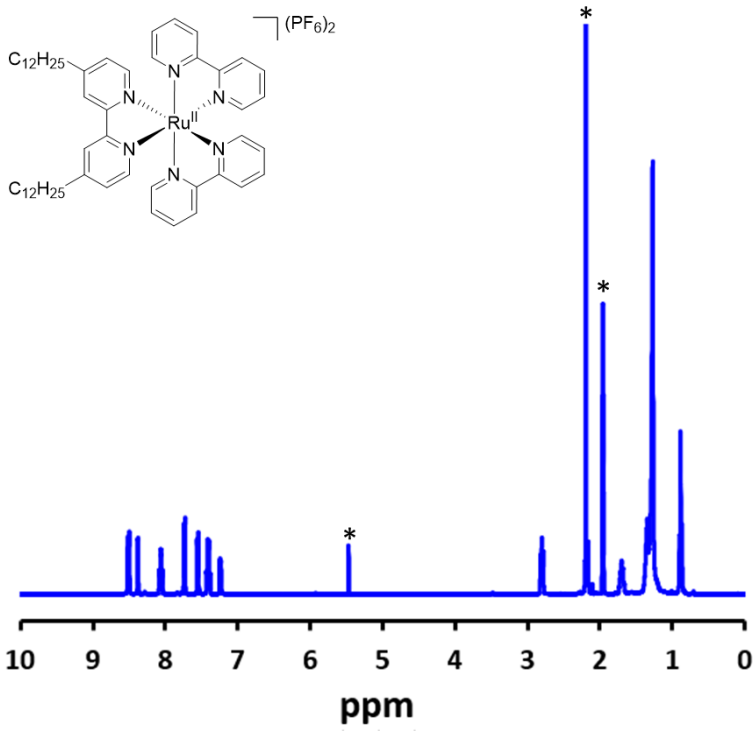

Figure S21. ^{1}H-NMR of **RuC$_{12}$** in CD_3CN. Solvent peaks are indicated with *.

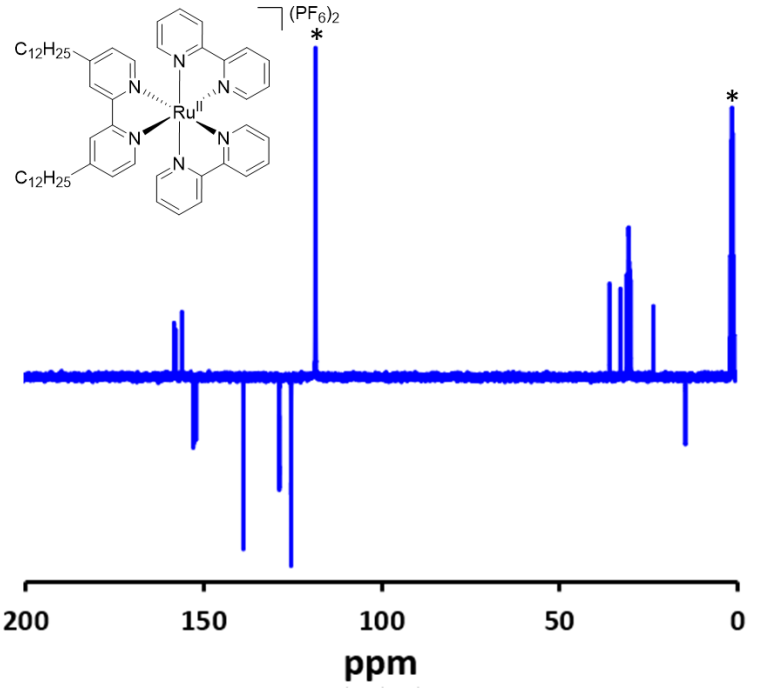

Figure S22. ^{13}C-NMR of **RuC$_{12}$** in CD_3CN. Solvent peaks are indicated with *.

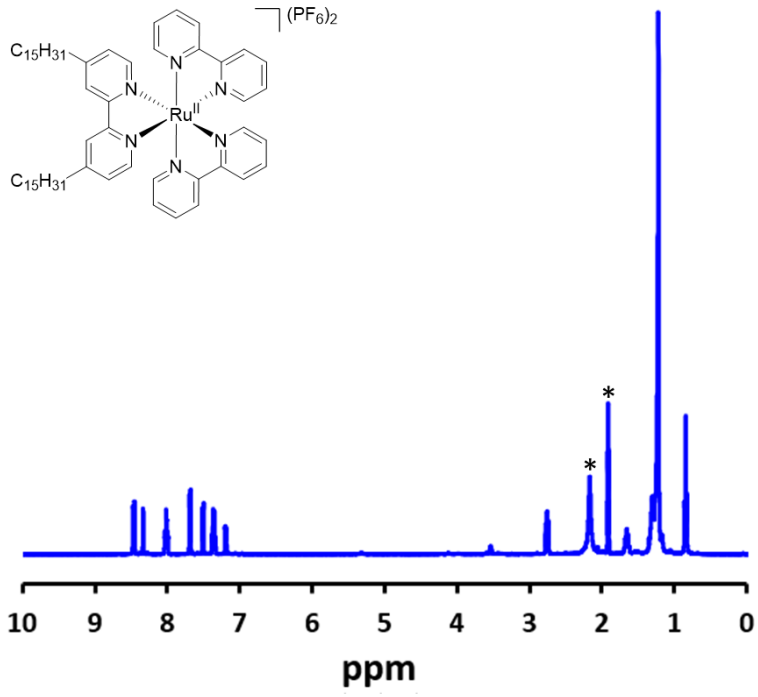

Figure S23. ^{1}H-NMR of **RuC$_{15}$** in CD_3CN. Solvent peaks are indicated with *.

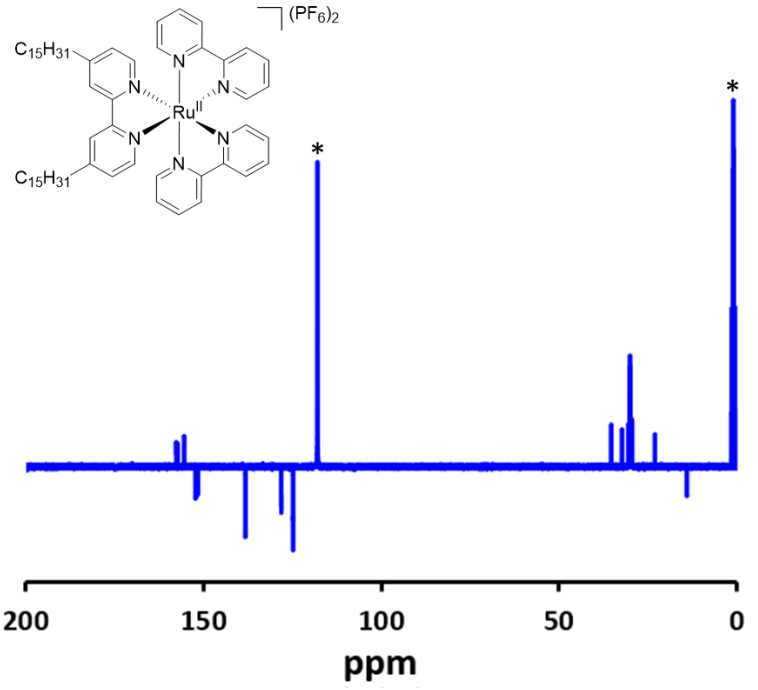

Figure S24. ^{13}C-NMR of **RuC$_{15}$** in CD_3CN. Solvent peaks are indicated with *.

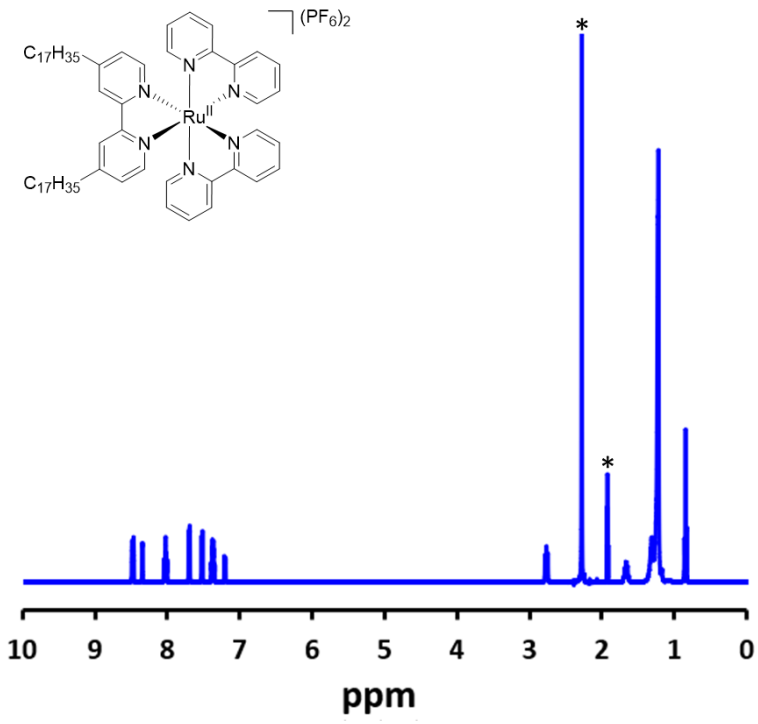

Figure S25. ^{1}H-NMR of **RuC$_{17}$** in CD_3CN. Solvent peaks are indicated with *.

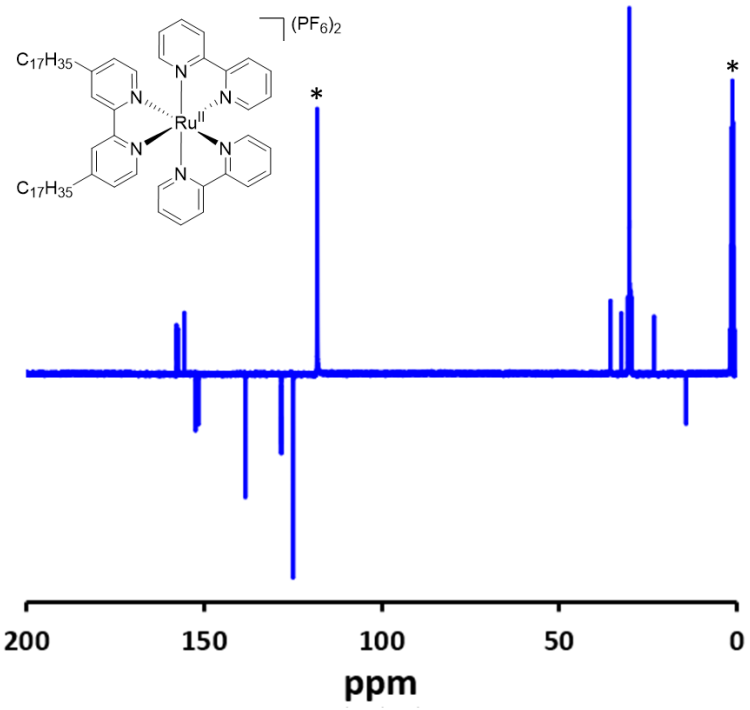

Figure S26. ^{13}C-NMR of **RuC$_{17}$** in CD_3CN. Solvent peaks are indicated with *.

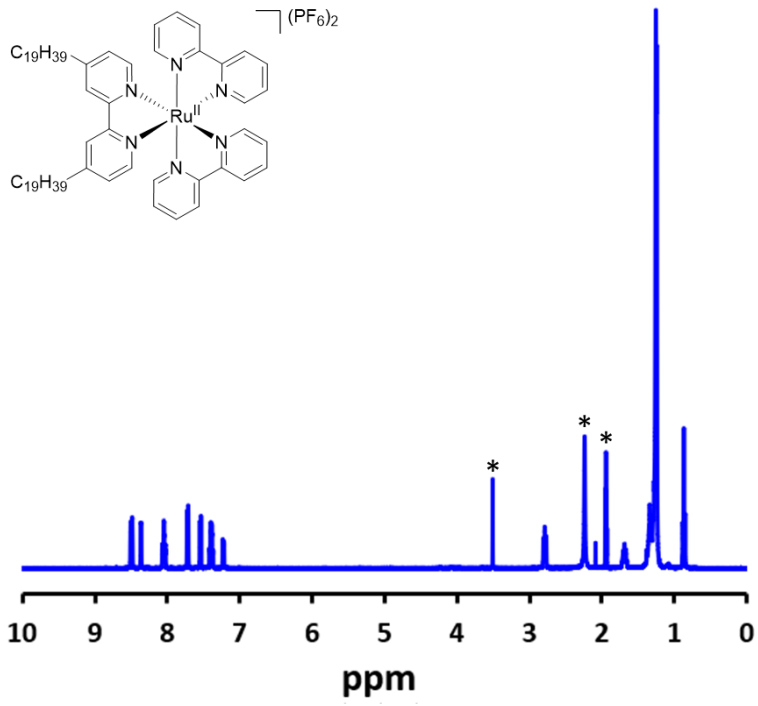

Figure S27. ^{1}H-NMR of **RuC$_{19}$** in CD_3CN. Solvent peaks are indicated with *.

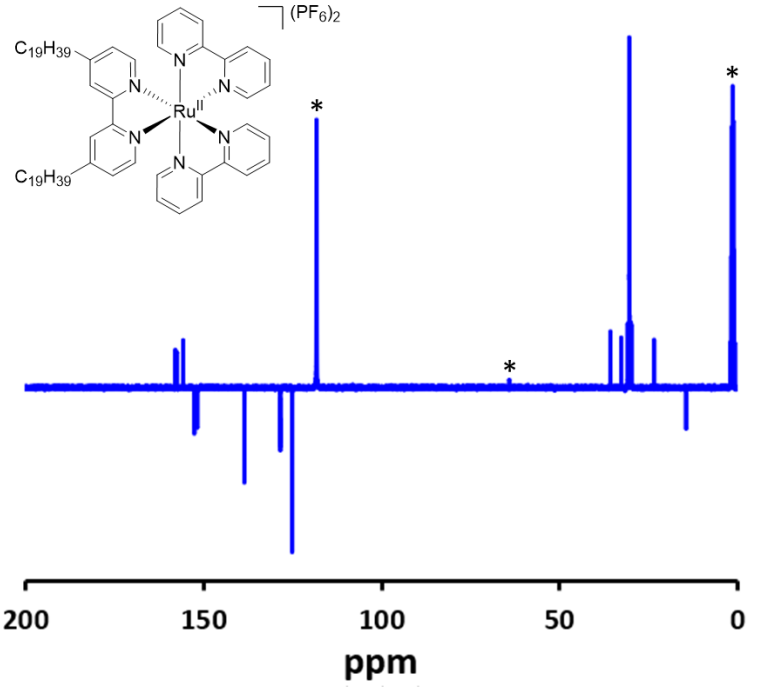

Figure S28. ^{13}C-NMR of **RuC$_{19}$** in CD_3CN. Solvent peaks are indicated with *.

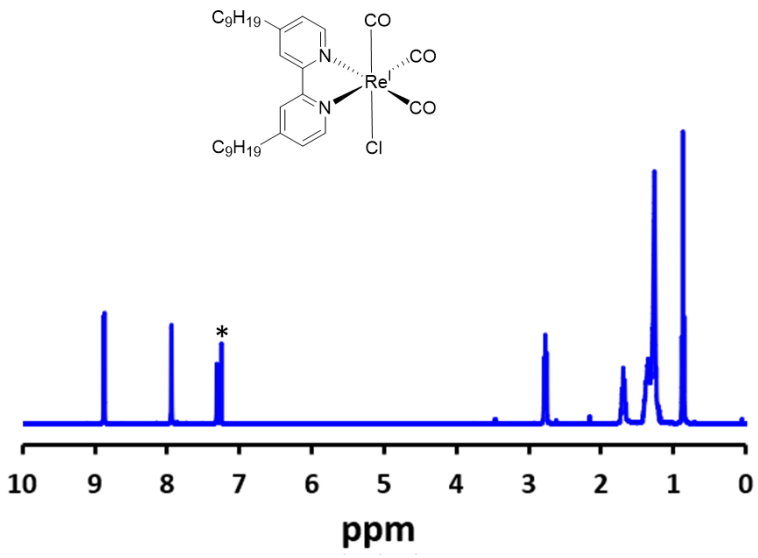

Figure S29. ^{1}H-NMR of **ReC$_9$** in $CDCl_3$. Solvent peaks are indicated with *.

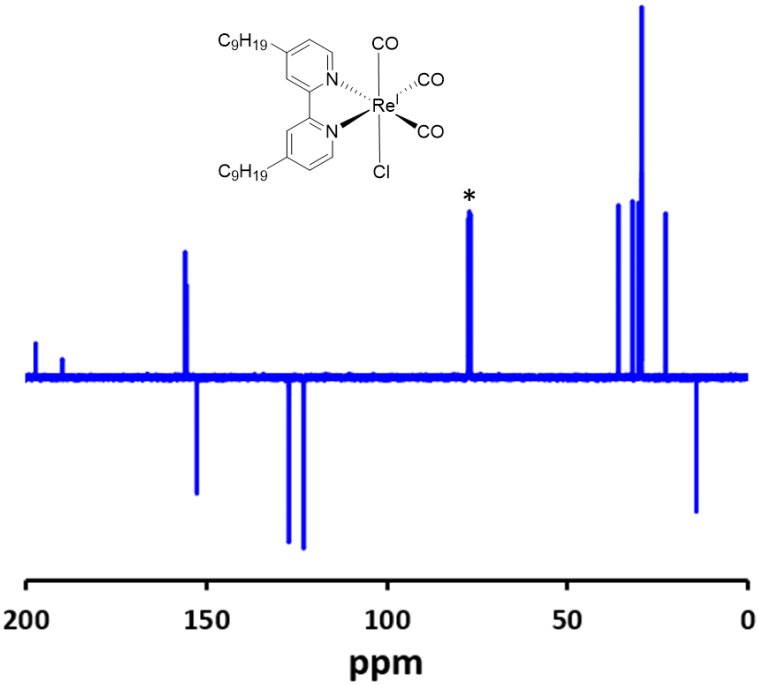

Figure S30. ^{13}C-NMR of **ReC$_9$** in $CDCl_3$. Solvent peaks are indicated with *.

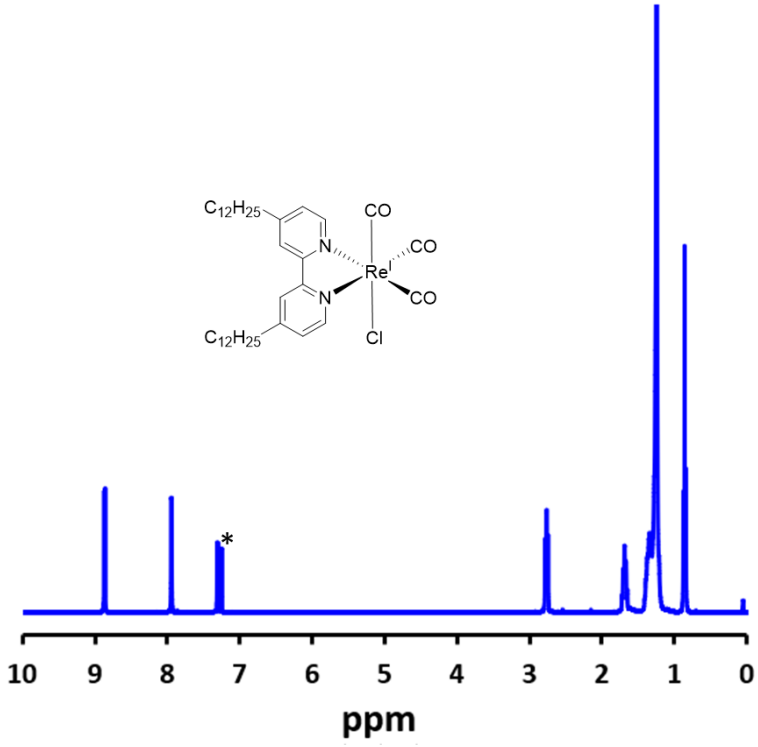

Figure S31. ^{1}H-NMR of **ReC$_{12}$** in $CDCl_3$. Solvent peaks are indicated with *.

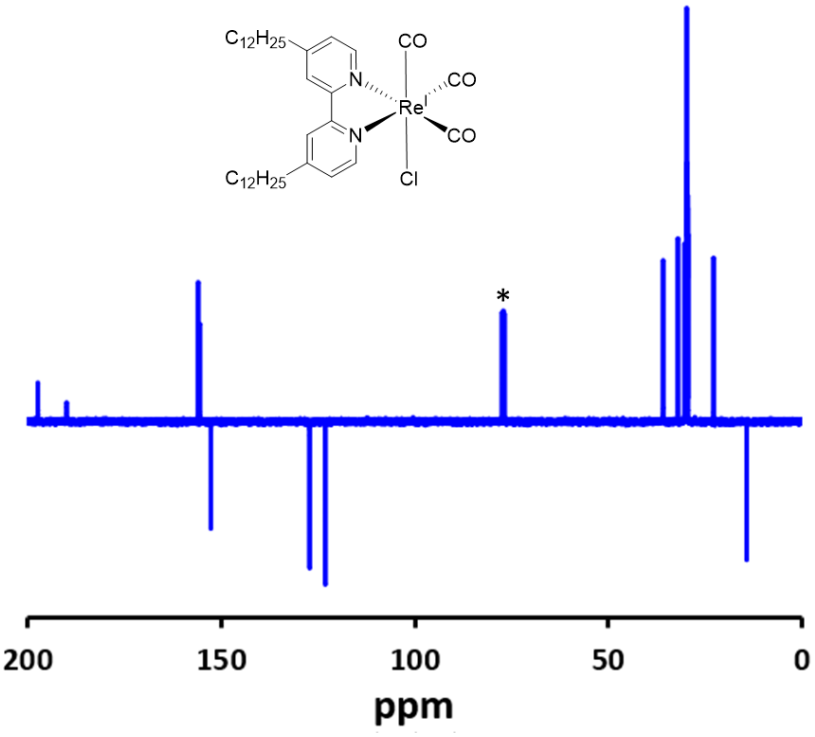

Figure S32. ^{13}C-NMR of **ReC$_{12}$** in $CDCl_3$. Solvent peaks are indicated with *.

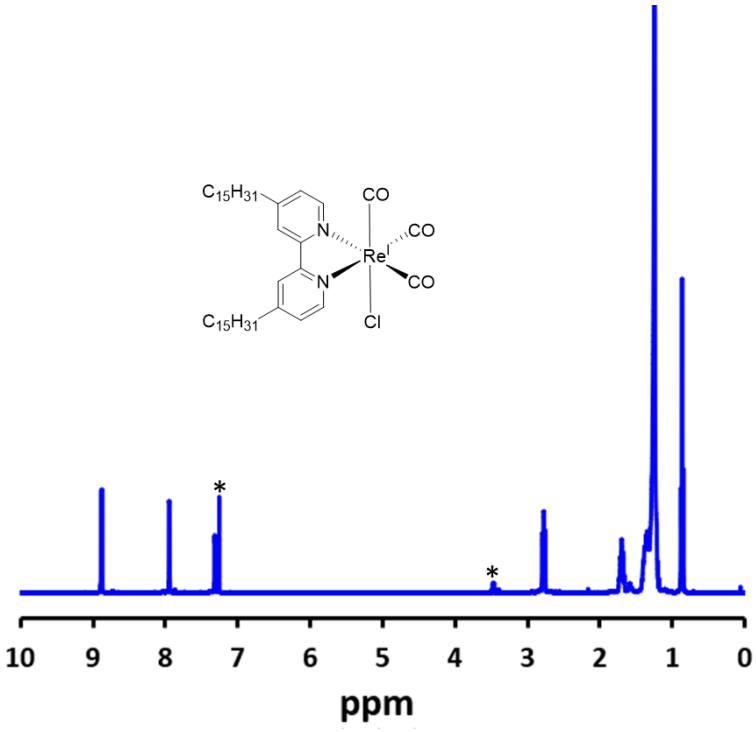

Figure S33. ^{1}H-NMR of **ReC$_{15}$** in $CDCl_3$. Solvent peaks are indicated with *.

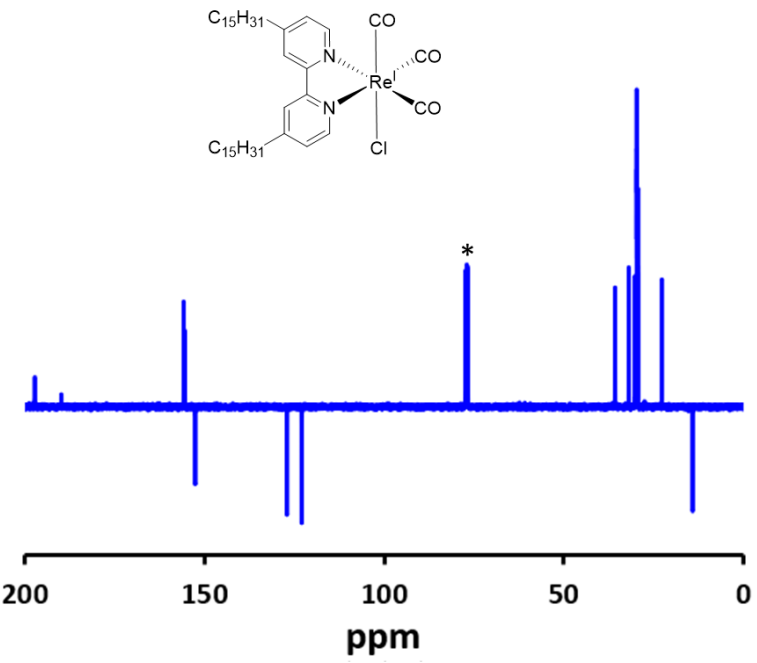

Figure S34. ^{13}C-NMR of **ReC$_{15}$** in $CDCl_3$. Solvent peaks are indicated with *.

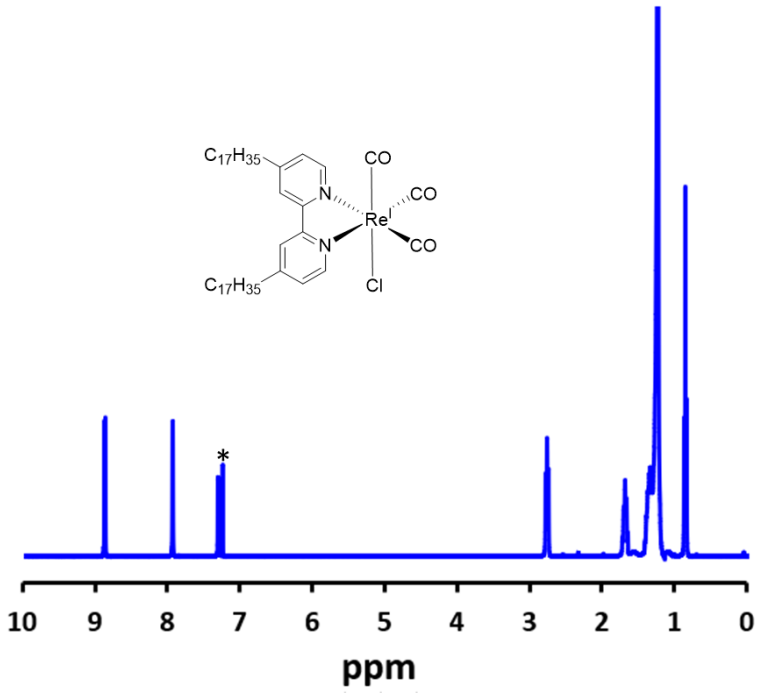

Figure S35. ^{1}H-NMR of **ReC$_{17}$** in $CDCl_3$. Solvent peaks are indicated with *.

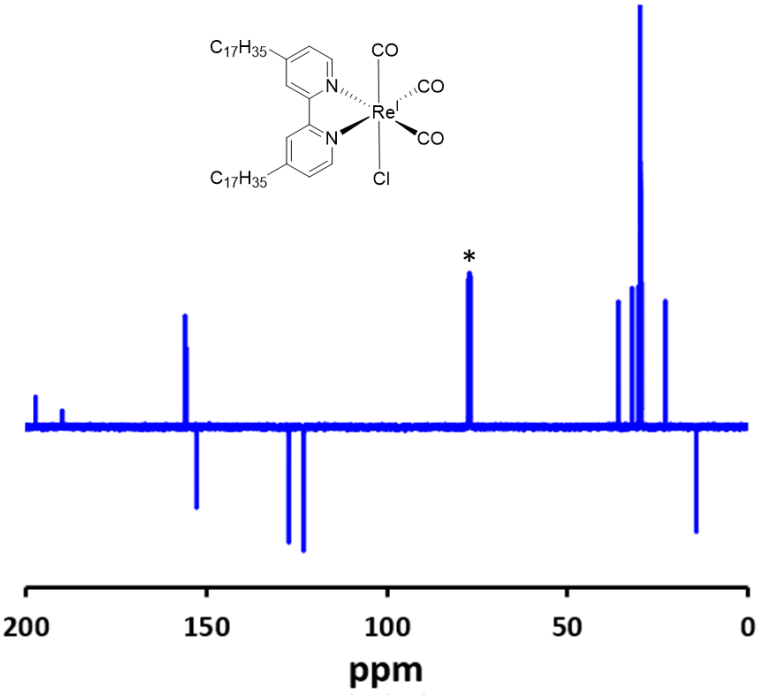

Figure S36. ^{13}C-NMR of **ReC$_{17}$** in $CDCl_3$. Solvent peaks are indicated with *.

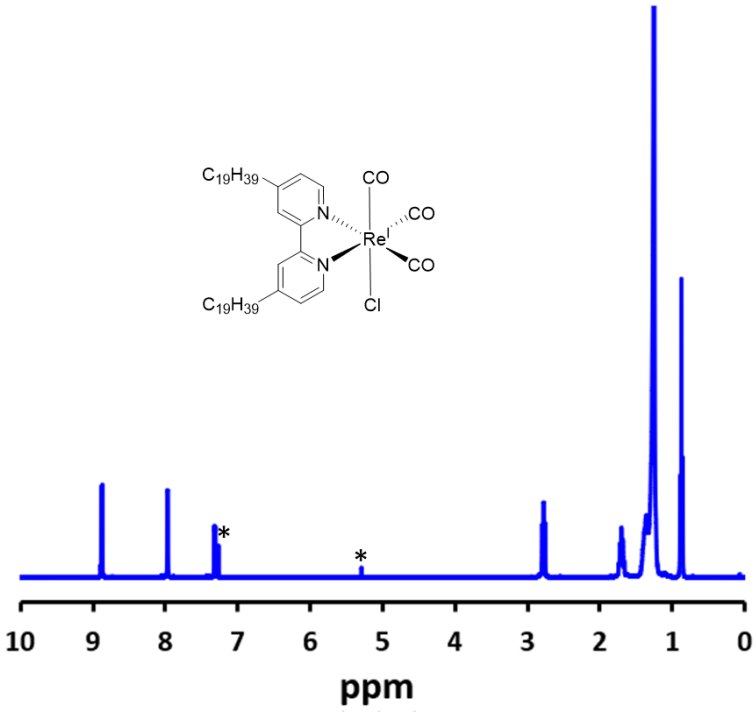

Figure S37. ^{1}H-NMR of **ReC$_{19}$** in $CDCl_3$. Solvent peaks are indicated with *.

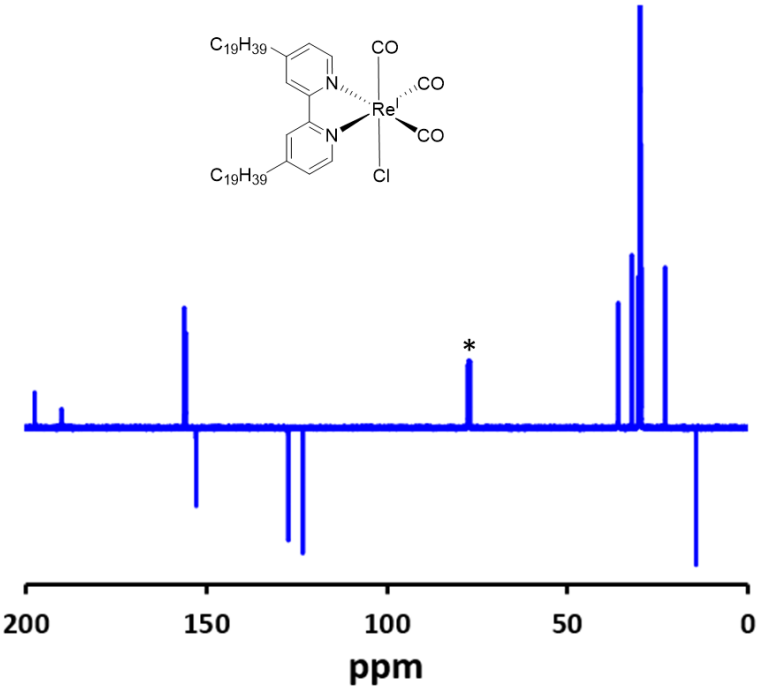

Figure S38. ^{13}C-NMR of ReC_{19} in $CDCl_3$. Solvent peaks are indicated with *.

11. References

[1] J. J. Snellenburg, S. Laptenok, R. Seger, K. M. Mullen, I. H. M. van Stokkum, *J. Stat. Softw.* **2012**, *49*, 1–22.

[2] M. W. H. Hoorens, M. Medved', A. D. Laurent, M. Di Donato, S. Fanetti, L. Slappendel, M. Hilbers, B. L. Feringa, W. J. Buma, W. Szymanski, *Nat. Commun.* **2019**, *10*, 2390.

[3] G. B. Berselli, N. K. Sarangi, S. Ramadurai, P. V Murphy, T. E. Keyes, *ACS Appl. Bio Mater.* **2019**, *2*, 3404–3417.

[4] J. E. Collins, J. J. S. Lamba, J. C. Love, J. E. McAlvin, C. Ng, B. P. Peters, X. Wu, C. L. Fraser, *Inorg. Chem.* **1999**, *38*, 2020–2024.

[5] K. Neuthe, F. Bittner, F. Stiemke, B. Ziem, J. Du, M. Zellner, M. Wark, T. Schubert, R. Haag, *Dyes Pigm.* **2014**, *104*, 24–33.

[6] L. A. Worl, R. Duesing, P. Chen, L. Della Ciana, T. J. Meyer, *J. Chem. Soc. Dalt. Trans.* **1991**, 849–858.

[7] N. Ikuta, S. Y. Takizawa, S. Murata, *Photochem. Photobiol. Sci.* **2014**, *13*, 691–702.

[8] B. Limburg, E. Bouwman, S. Bonnet, *J. Phys. Chem. B* **2016**, *120*, 6969–6975.

[9] R. S. Khnayzer, V. S. Thoi, M. Nippe, A. E. King, J. W. Jurss, K. A. El Roz, J. R. Long, C. J. Chang, F. N. Castellano, *Energy Environ. Sci.* **2014**, *7*, 1477–1488.

[10] G. M. Sheldrick, *Acta Crystallogr. Sect. C* **2015**, *71*, 3–8.

[11] R. C. Clark, J. S. Reid, *Acta Crystallogr. Sect. A* **1995**, *51*, 887–897.

[12] G. M. Sheldrick, *Acta Crystallogr. Sect. A* **2008**, *64*, 112–122.